

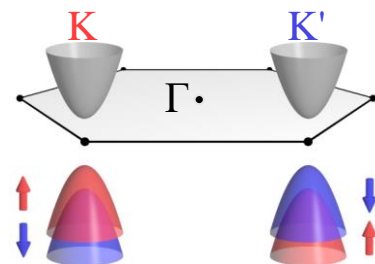
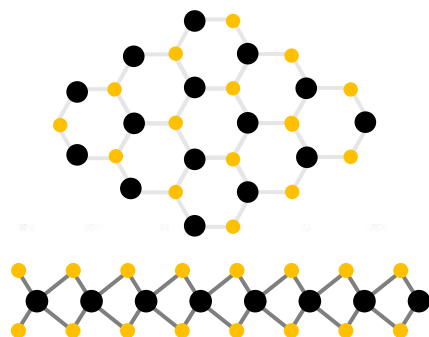
Hybrid moiré excitons and trions

Anvar Baimuratov

Monolayer 2D semiconductors

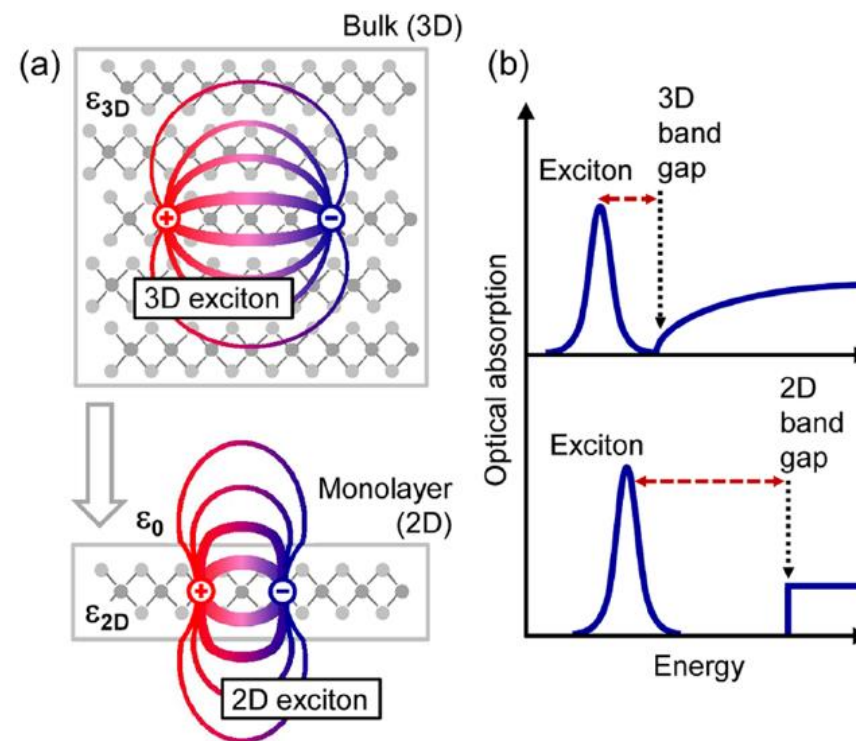
Transition Metal Dichalcogenides:

MoS₂
 MoSe₂
 MoTe₂
 WS₂
 WSe₂



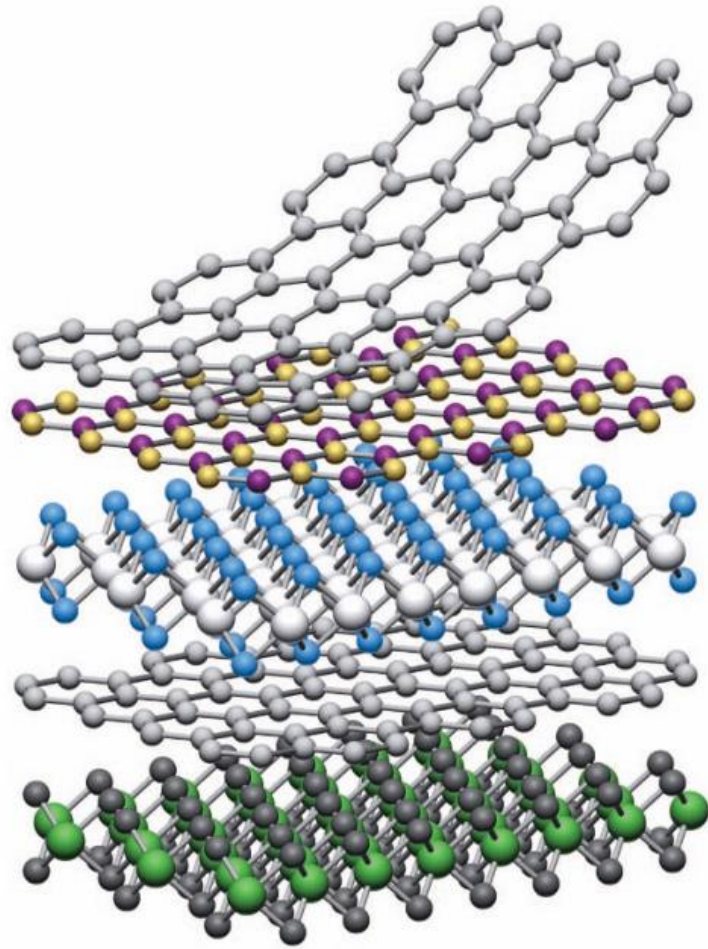
hydrogen 1 H 1.0079																	helium 2 He 4.0026	
lithium 3 Li 6.941	beryllium 4 Be 9.0122																	neon 10 Ne 20.180
sodium 11 Na 22.990	magnesium 12 Mg 24.305																	argon 18 Ar 39.948
potassium 19 K 39.098	calcium 20 Ca 40.078	scandium 21 Sc 44.956	titanium 22 Ti 47.867	vanadium 23 V 50.942	chromium 24 Cr 51.996	manganese 25 Mn 54.938	iron 26 Fe 55.845	cobalt 27 Co 58.933	nickel 28 Ni 58.693	copper 29 Cu 63.546	zinc 30 Zn 65.39	gallium 31 Ga 69.723	germanium 32 Ge 72.61	arsenic 33 As 74.922	sele 34 Se 78.96	bromine 35 Br 79.904	krypton 36 Kr 83.80	
rubidium 37 Rb 85.468	strontium 38 Sr 87.62	yttrium 39 Y 88.906	zirconium 40 Zr 91.224	niobium 41 Nb 92.906	niobium 42 Mo 95.94	technetium 43 Tc [98]	ruthenium 44 Ru 101.07	rhodium 45 Rh 106.42	palladium 46 Pd 107.87	silver 47 Ag 107.87	cadmium 48 Cd 112.41	indium 49 In 114.82	tin 50 Sn 118.71	antimony 51 Sb 121.76	tellurium 52 Te 127.60	iodine 53 I 126.90	xenon 54 Xe 131.29	
cesium 55 Cs 132.91	barium 56 Ba 137.33	lutetium 71 Lu 174.97	hafnium 72 Hf 178.49	tantalum 73 Ta 180.95	tungsten 74 W 183.84	rhenium 75 Re 186.21	osmium 76 Os 190.23	iridium 77 Ir 192.22	platinum 78 Pt 195.08	gold 79 Au 196.97	mercury 80 Hg 200.59	thallium 81 Tl 204.38	lead 82 Pb 207.2	bismuth 83 Bi 208.98	polonium 84 Po [209]	astatine 85 At [210]	radon 86 Rn [222]	
francium 87 Fr [223]	radium 88 Ra [226]	lawrencium 103 Lr [262]	rutherfordium 104 Rf [261]	dubnium 105 Db [262]	seaborgium 106 Sg [266]	bohrium 107 Bh [264]	hassium 108 Hs [269]	meitnerium 109 Mt [268]	unnilium 110 Uun [271]	ununium 111 Uuu [272]	unubium 112 Uub [277]	ununquadium 114 Uuq [289]						

- Direct semiconductors at K valleys
- Huge exciton binding energies

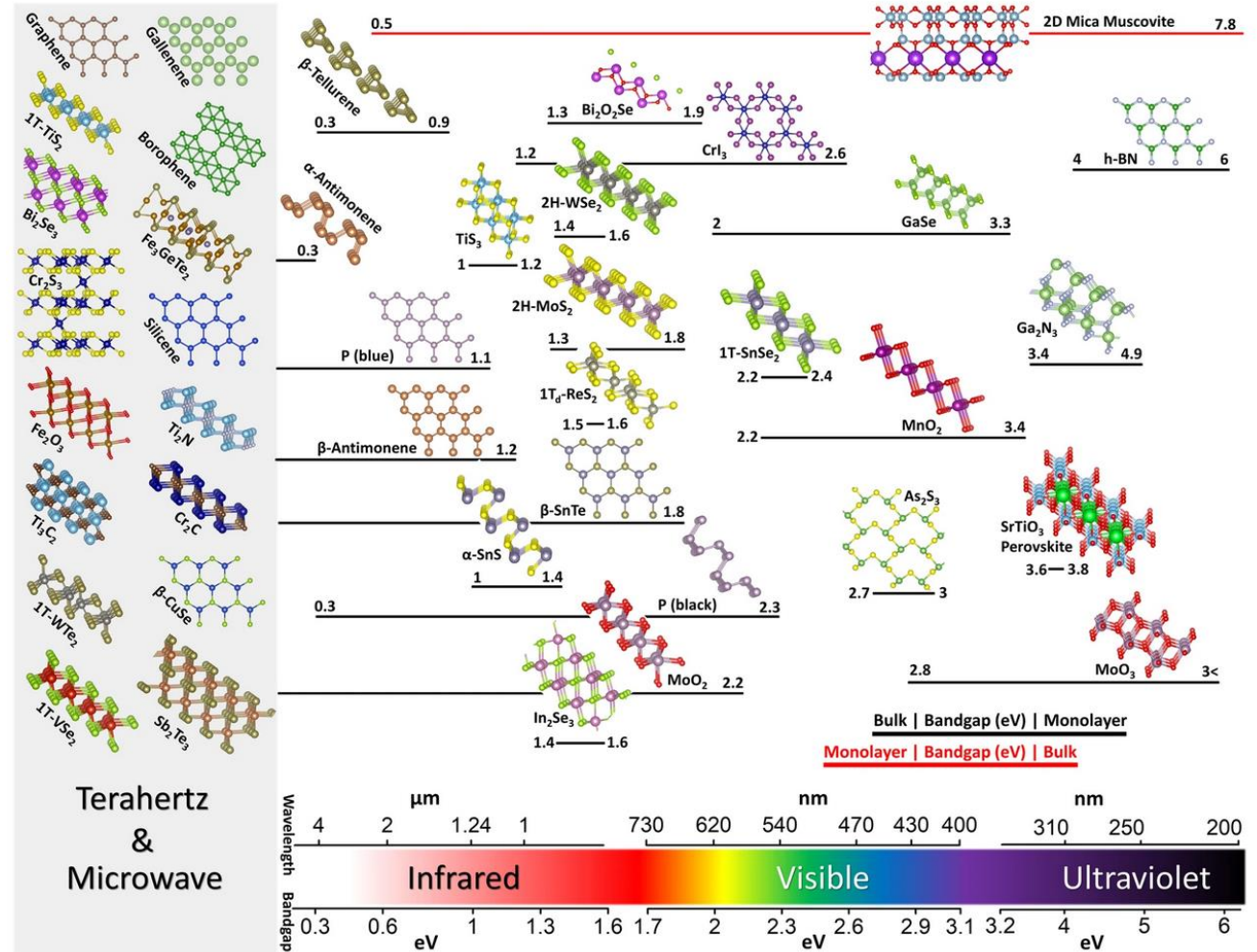


Chernikov et al., PRL 113, 076802 (2014)

van der Waals Lego for material engineering

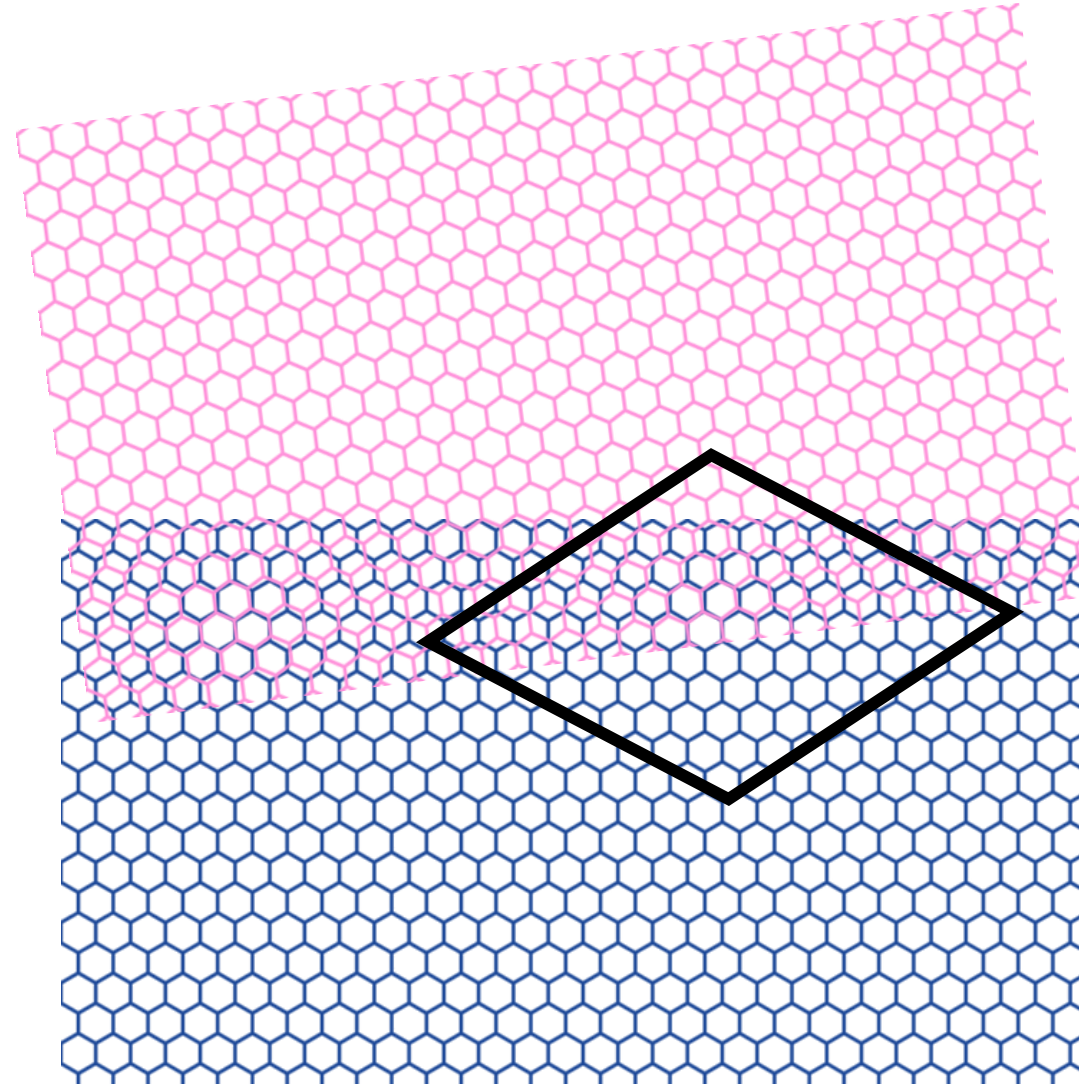


Geim et al., Nature 499, 419 (2013)

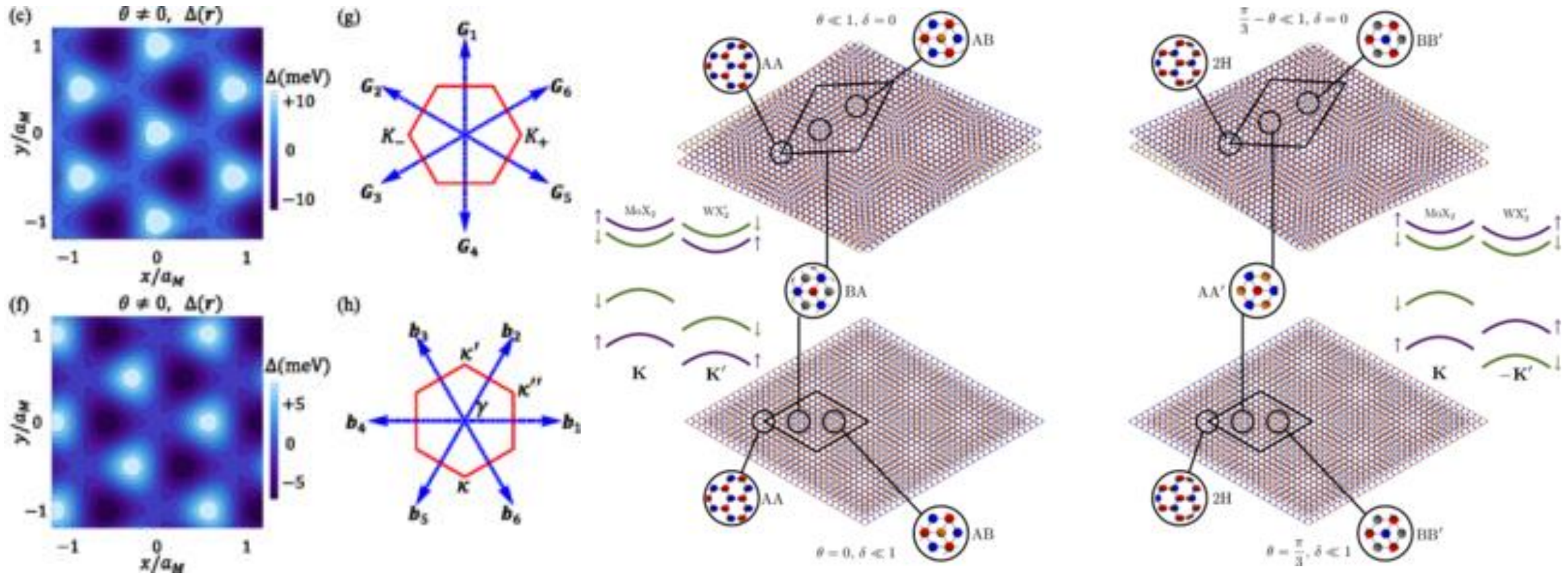


Chaves et al., npj 2D Mater. Appl. 4, 29 (2020)

Moiré superlattice formation in bilayers



Moiré theory



F. Wu, T. Lovorn, and A. H. MacDonald, PRL 118, 147401 (2017)

D. A. Ruiz-Tijerina and V. I. Fal'ko, PRB 99, 125424 (2019)

Heterobilayer MoSe₂/WS₂

- Lattice mismatch ~ 4%
- MoSe₂ and WS₂ have (almost) resonant CBs, allowing for intra- & interlayer exciton hybridization
- Holes are in MoSe₂ layer

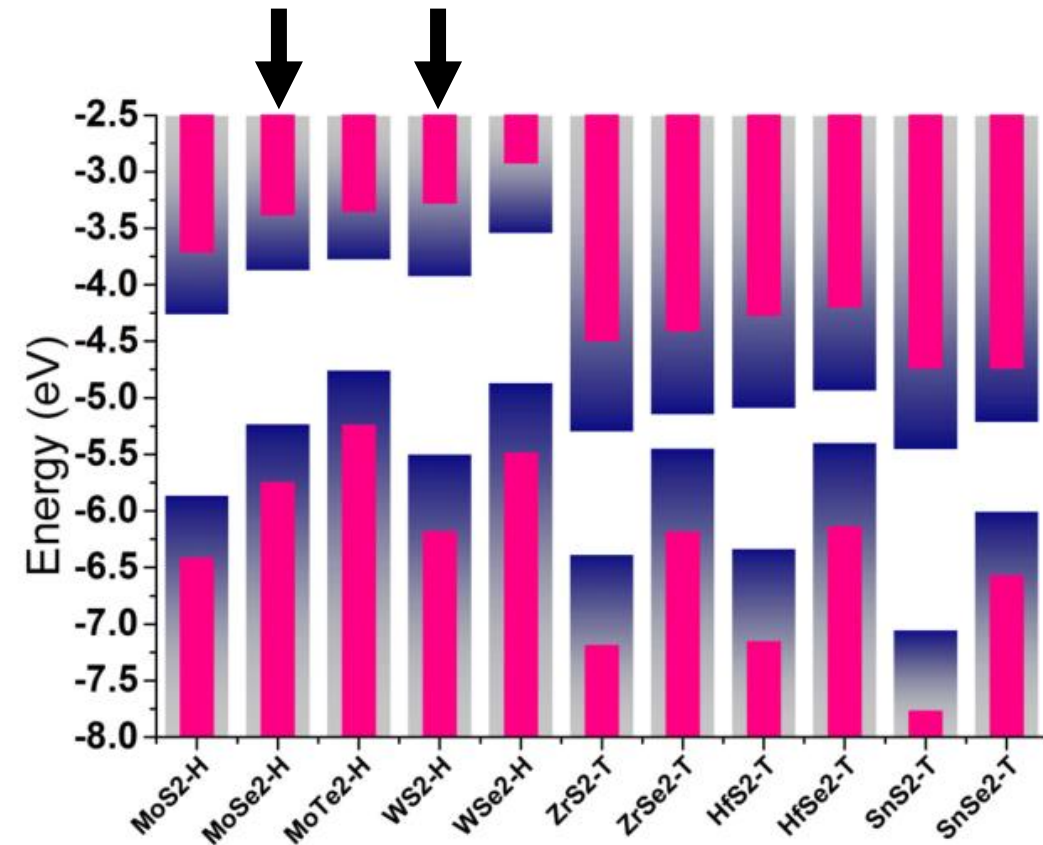
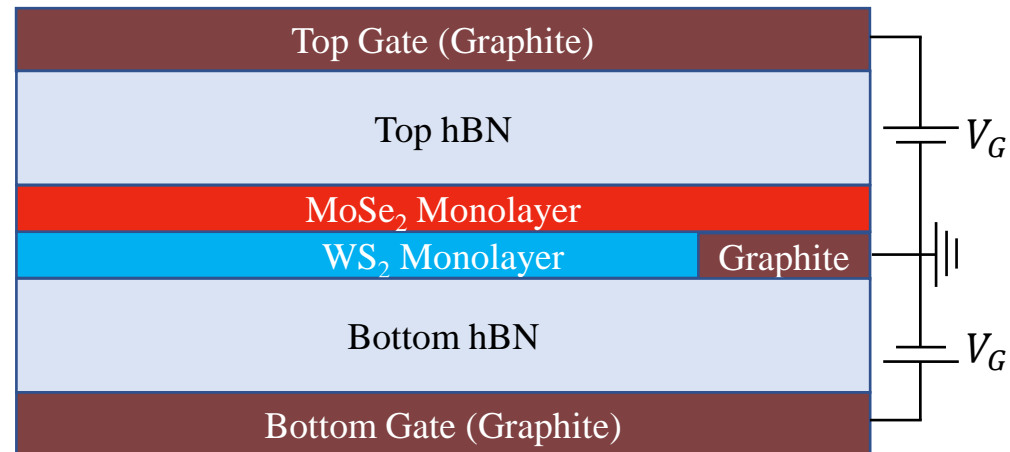


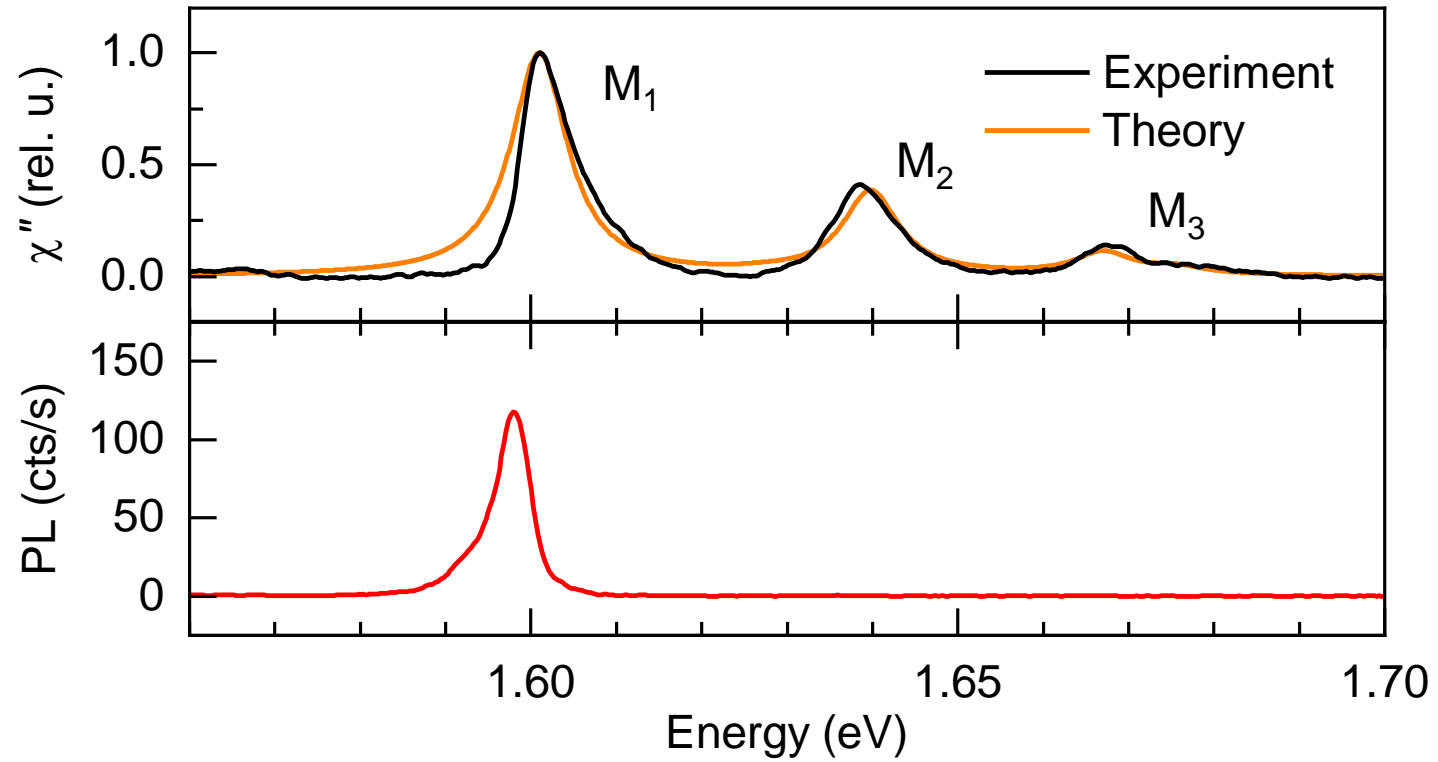
Figure 2. Position of band edges for stable semiconducting TMDs with respect to vacuum. The band edge of DFT-PBE data and G_0W_0 data are indicated by filled navy blue gradient column and pink solid column, respectively. The vacuum level is set to 0 eV.

Zhang et al., 2D Mater. 4, 015026 (2016)

Rotationally aligned MoSe₂/WS₂ in anti-parallel stacking (H-type) in a dual-gate field-effect device

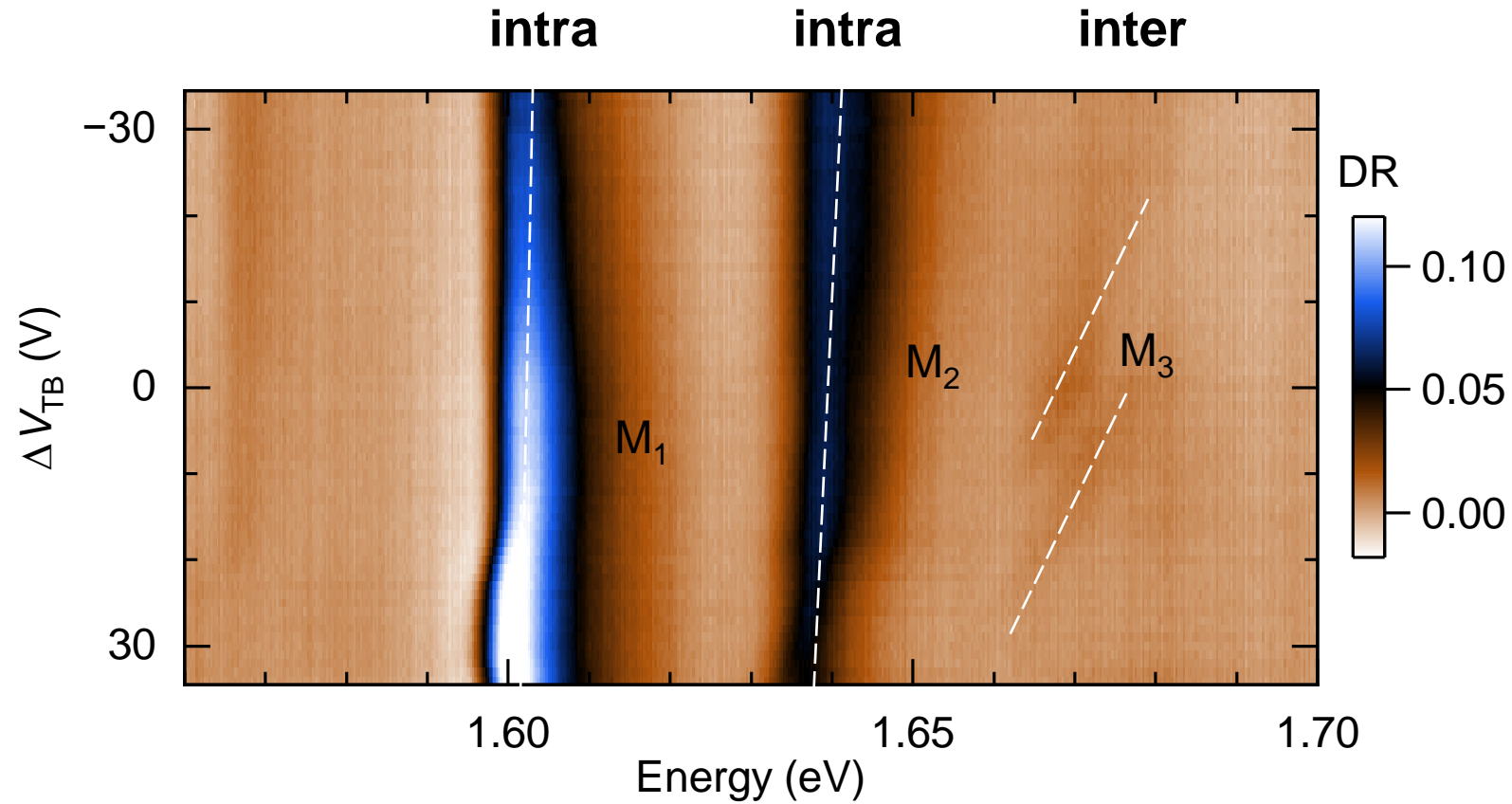


White-light DR and PL Data



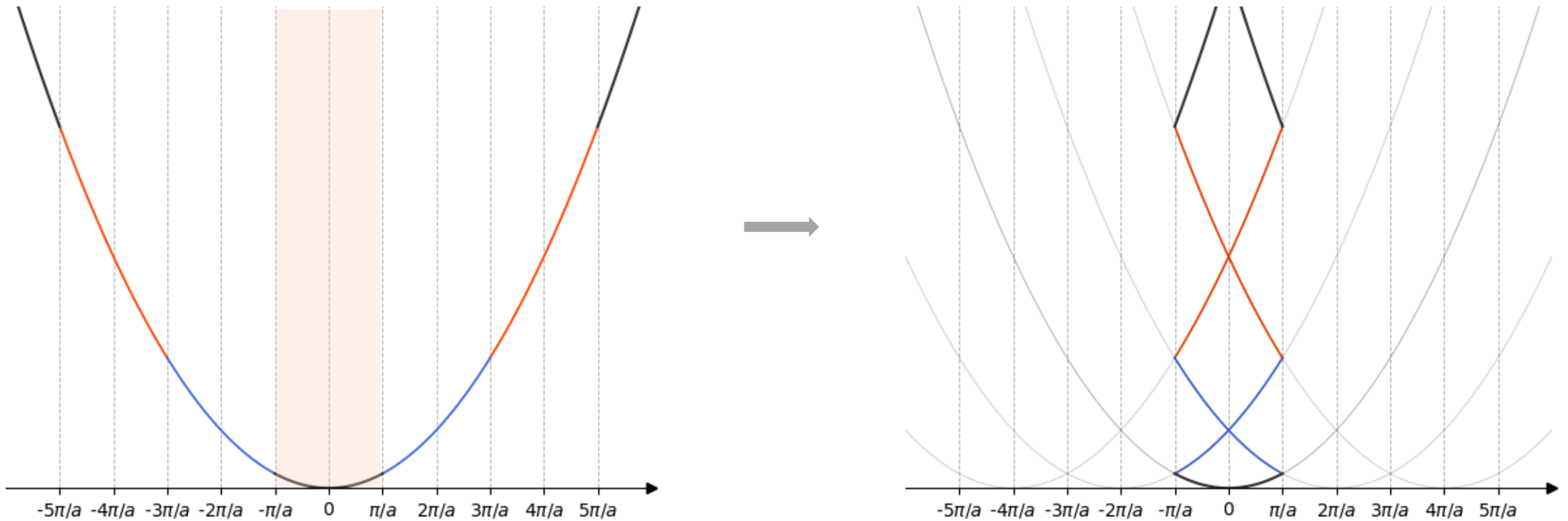
Polovnikov, ... , Baimuratov, PRL 32, 076902 (2024)

E-field dependence of white light DR

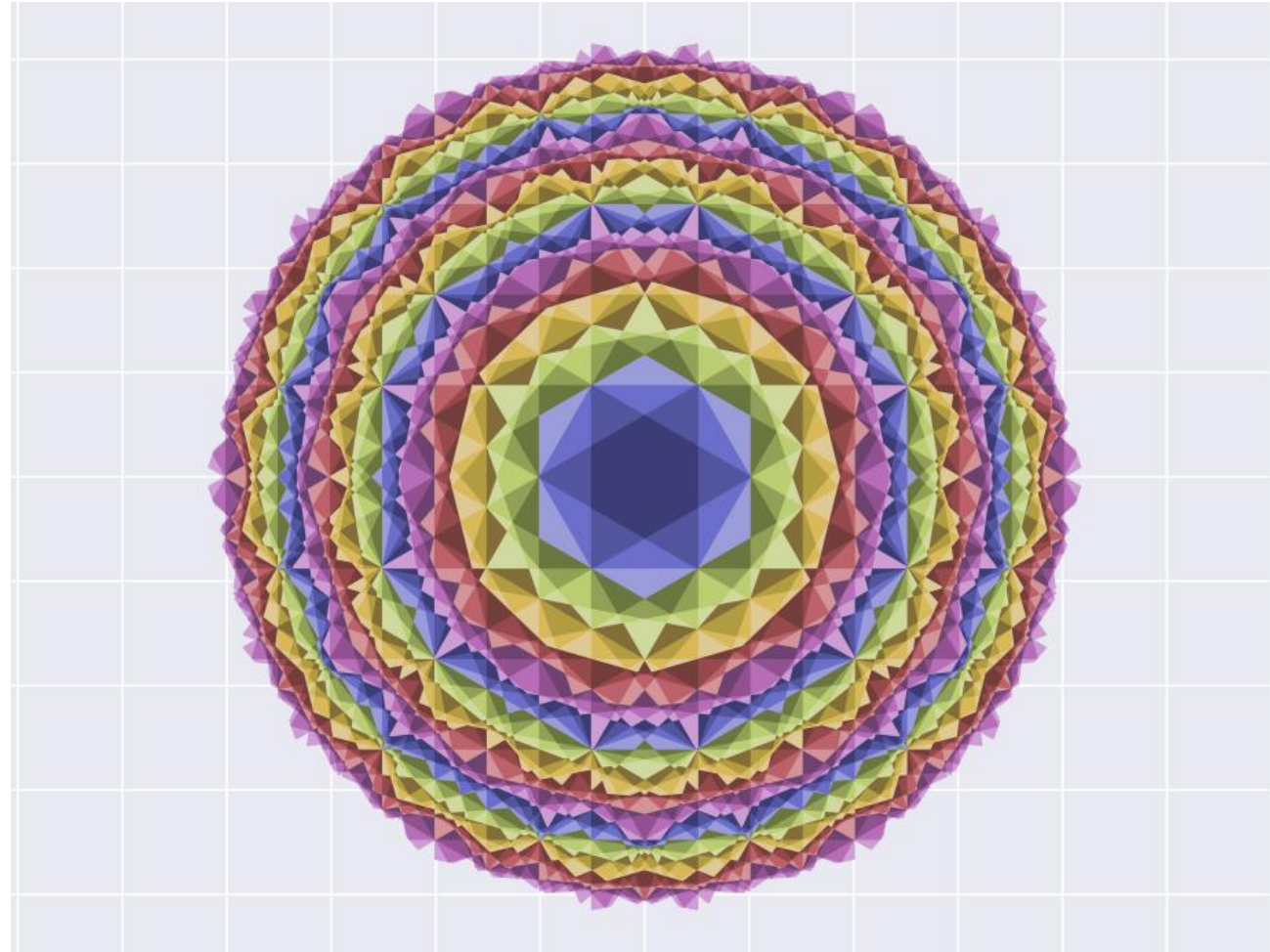


$$\Delta V_{TB} = V_B - V_T$$

Band folding in periodic lattices

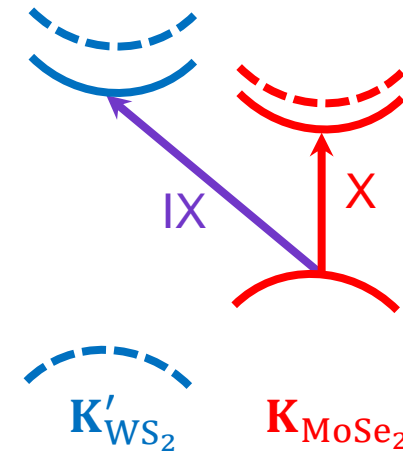
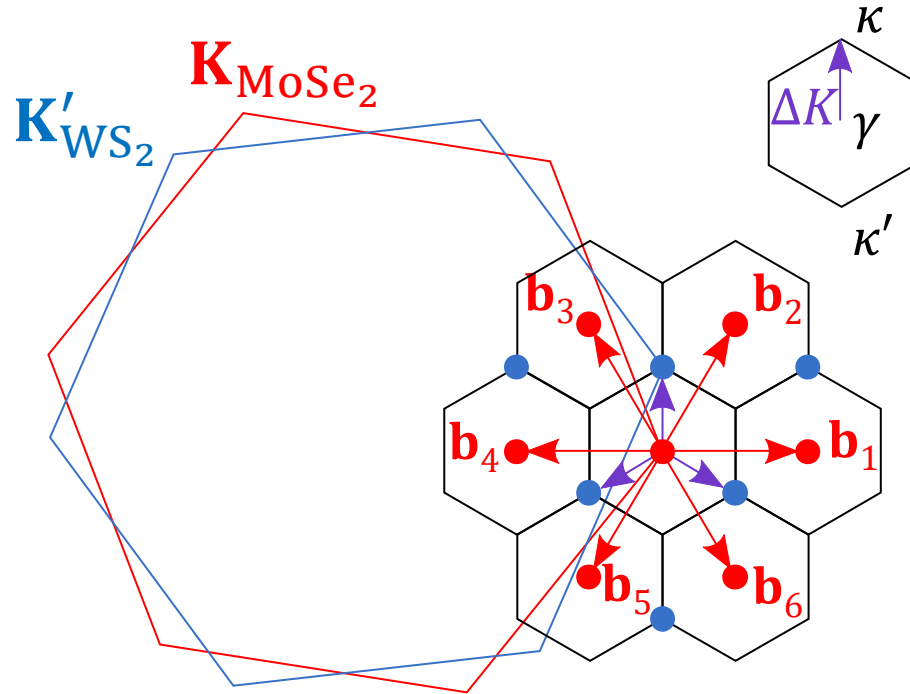


60 brillouin zones of a hexagonal lattice



<https://github.com/hamdav/brillouinzones>

Effective model for intra- and interlayer moiré excitons



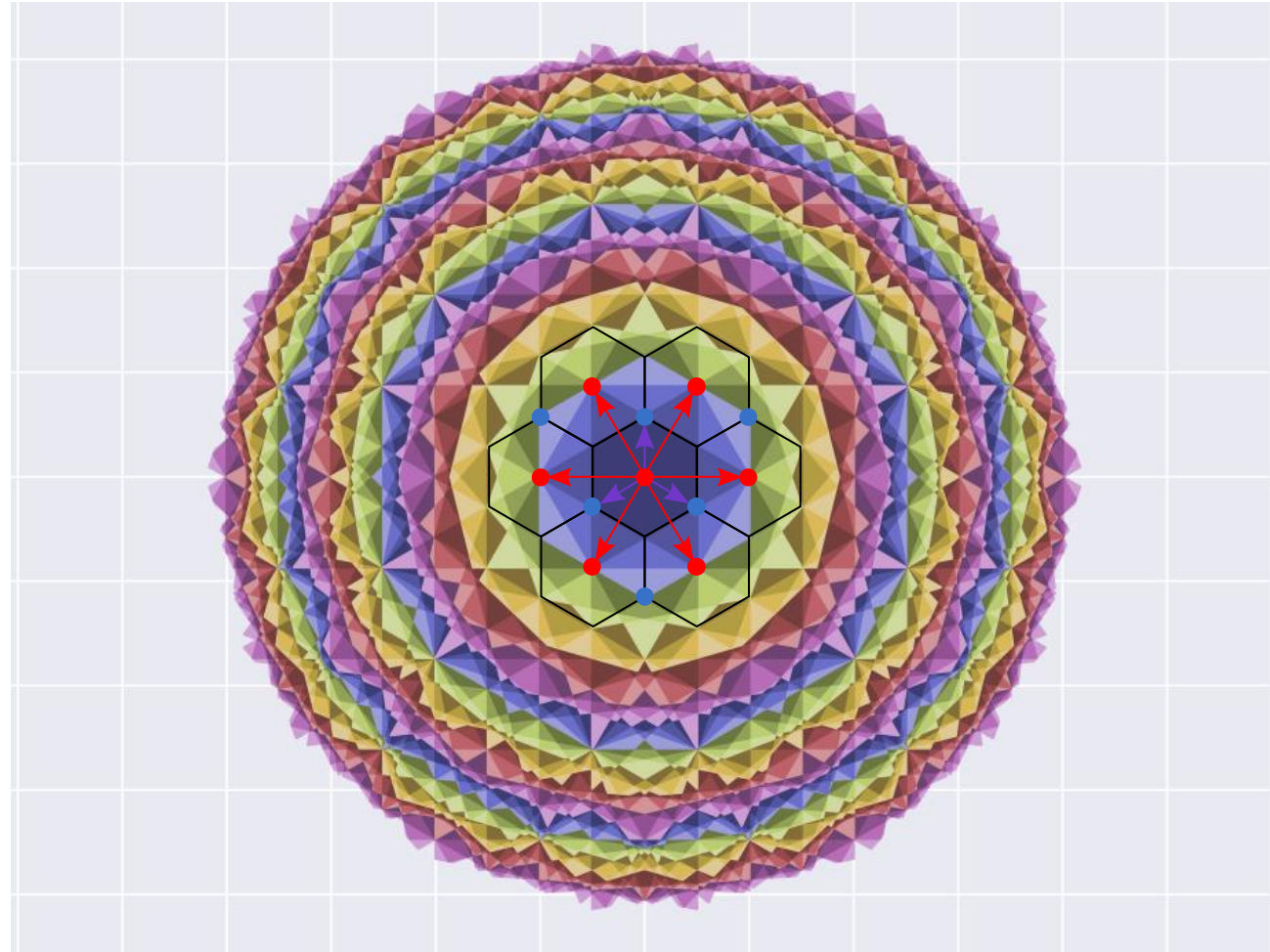
Intralayer
potential

$$V(\mathbf{r}) = \sum_{j=1}^6 V_j \exp(i\mathbf{b}_j \mathbf{r})$$

Interlayer
Coupling

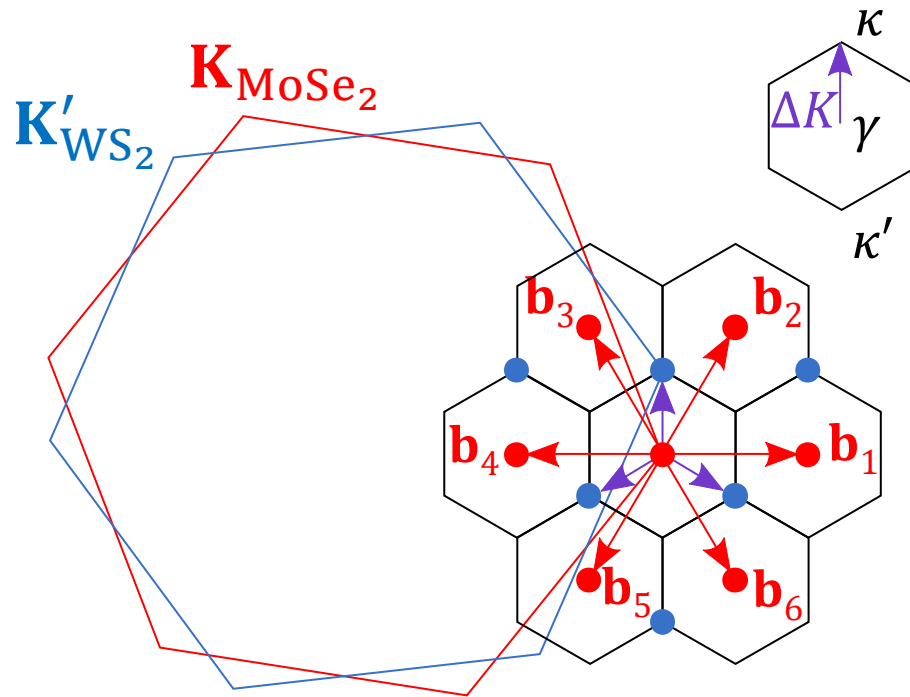
$$\langle IX, \mathbf{k}' + \mathbf{g}' | T | X, \mathbf{k} + \mathbf{g} \rangle = \sum_{\eta=0}^2 t \delta_{\mathbf{k} + \mathbf{g} - \mathbf{k}' - \mathbf{g}', C_3^\eta \Delta \mathbf{K}}$$

Four mini Brillouin zones



<https://github.com/hamdav/brillouinzones>

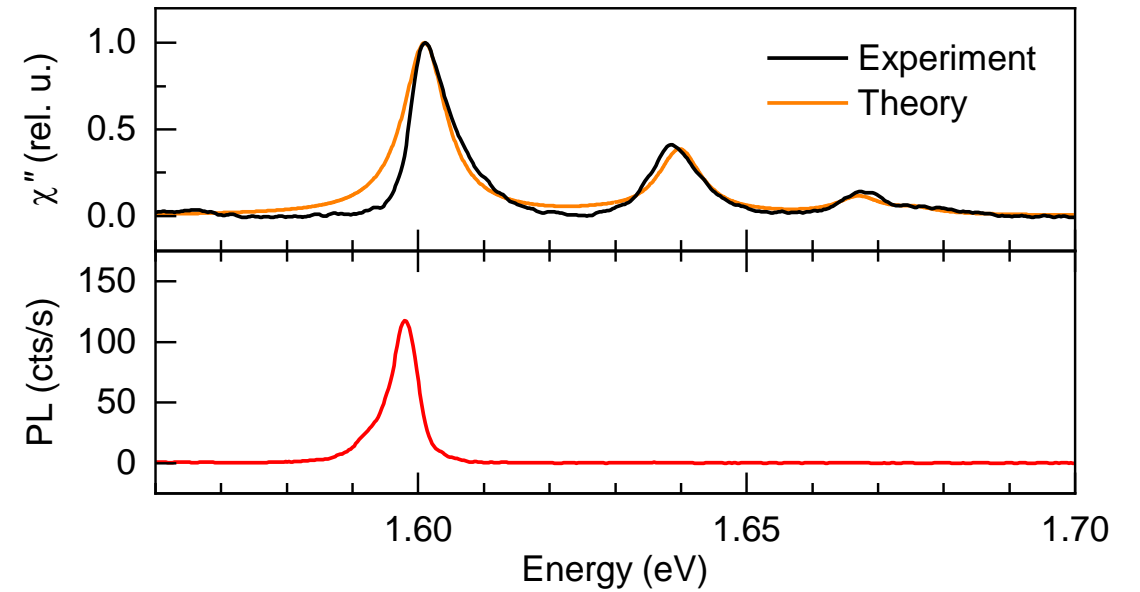
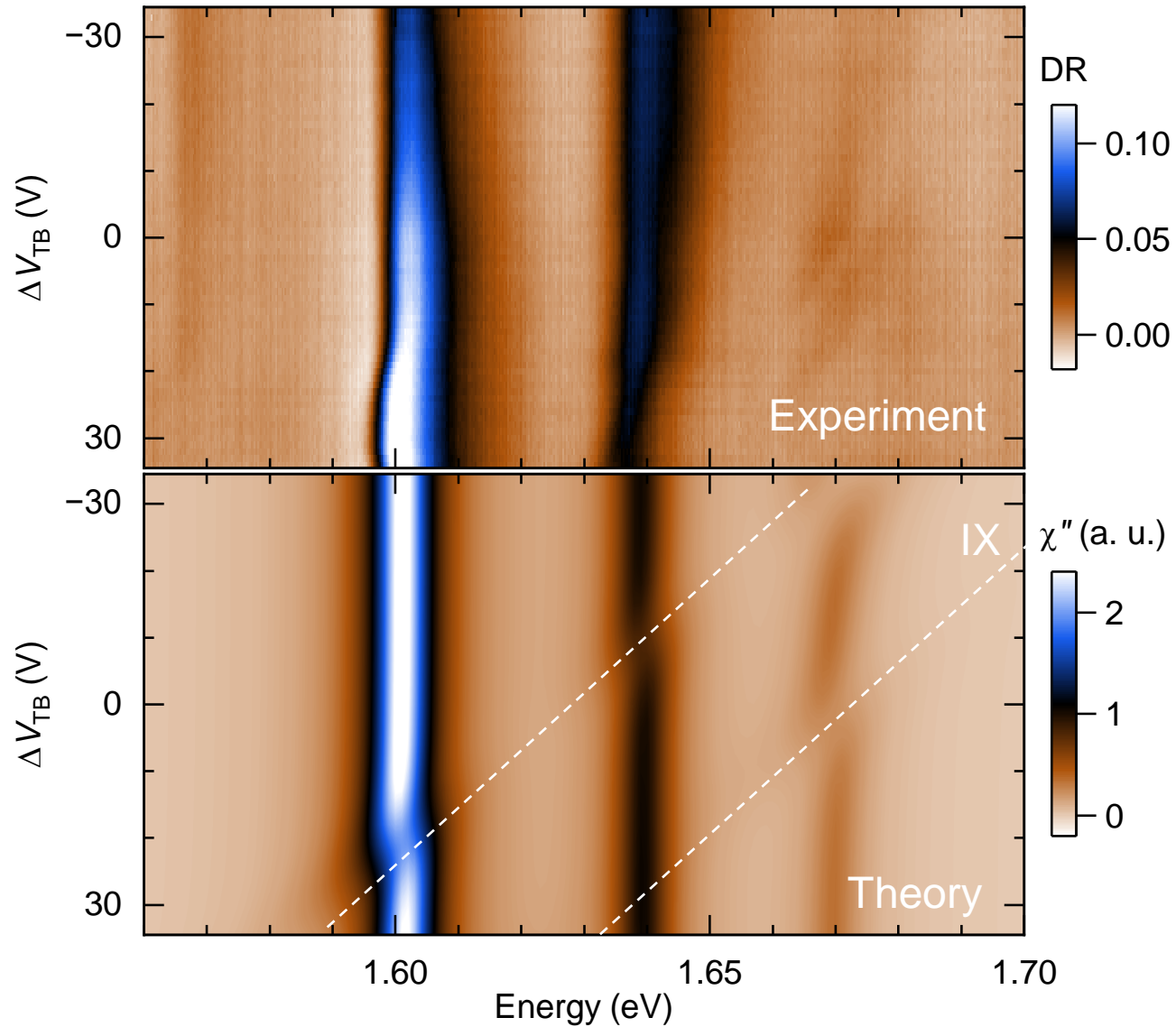
13-miniband Hamiltonian for moiré excitons



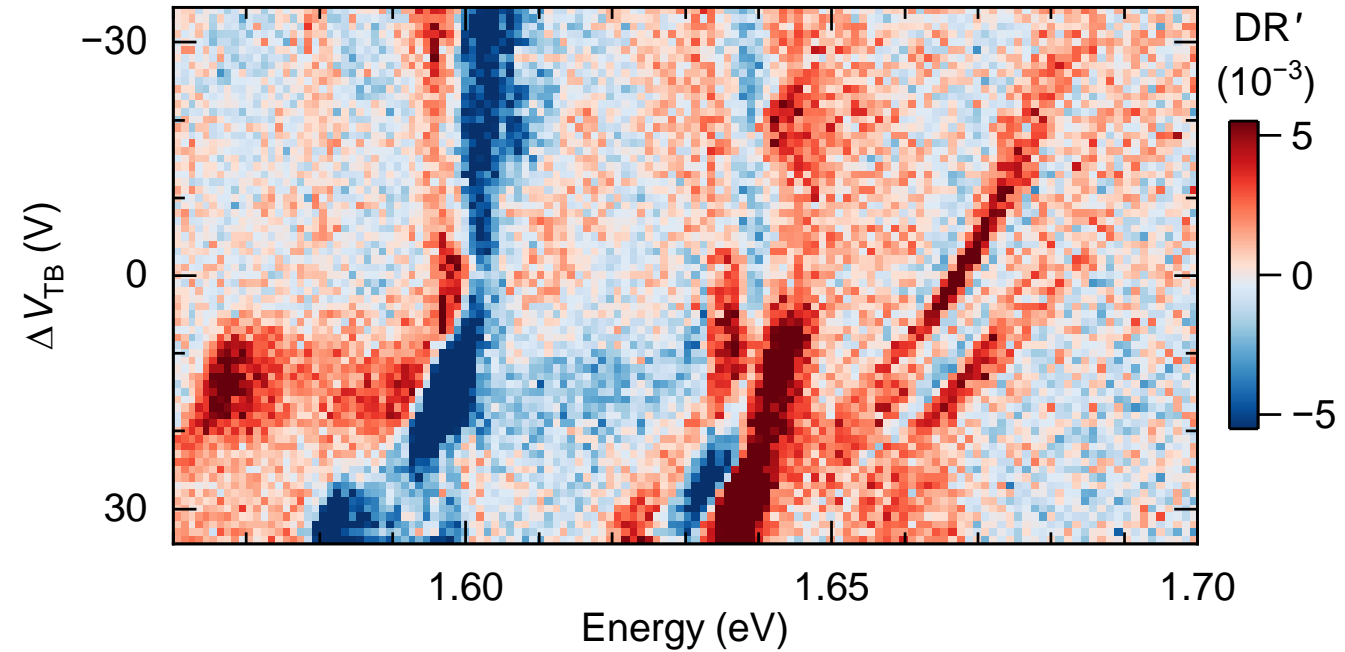
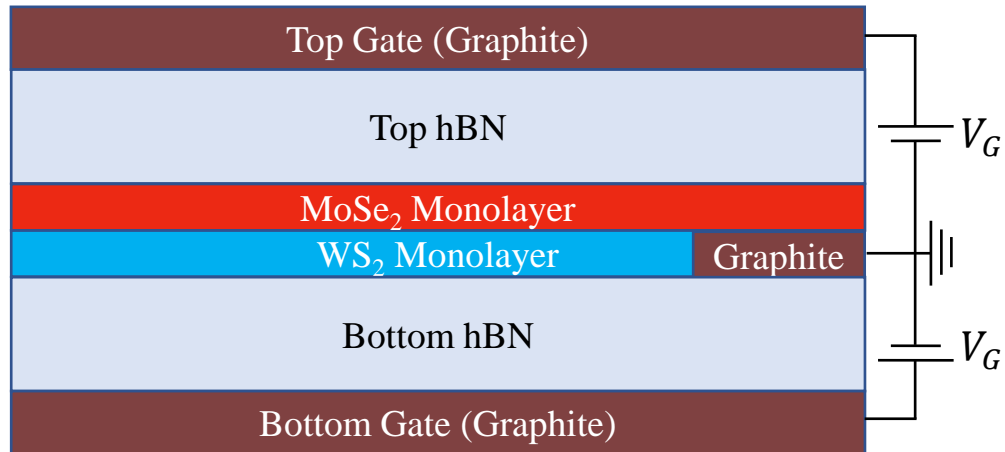
$H(\mathbf{k}) =$

$$\begin{pmatrix}
 E_0 & V & V^* & V & V^* & V & V^* & t & t & t & 0 & 0 & 0 \\
 V^* & E_1 & V & 0 & 0 & 0 & V & 0 & 0 & t & 0 & t & 0 \\
 V & V^* & E_2 & V^* & 0 & 0 & 0 & t & 0 & 0 & 0 & t & 0 \\
 V^* & 0 & V & E_3 & V & 0 & 0 & t & 0 & 0 & 0 & 0 & t \\
 V & 0 & 0 & V^* & E_4 & V^* & 0 & 0 & t & 0 & 0 & 0 & t \\
 V^* & 0 & 0 & 0 & V & E_5 & V & 0 & t & 0 & t & 0 & 0 \\
 V & V^* & 0 & 0 & 0 & V^* & E_6 & 0 & 0 & t & t & 0 & 0 \\
 t^* & 0 & t^* & t^* & 0 & 0 & 0 & \mathcal{E}_0 & 0 & 0 & 0 & 0 & 0 \\
 t^* & 0 & 0 & 0 & t^* & t^* & 0 & 0 & \mathcal{E}_1 & 0 & 0 & 0 & 0 \\
 t^* & t^* & 0 & 0 & 0 & 0 & t^* & 0 & 0 & \mathcal{E}_2 & 0 & 0 & 0 \\
 0 & 0 & 0 & 0 & 0 & t^* & t^* & 0 & 0 & 0 & \mathcal{E}_3 & 0 & 0 \\
 0 & t^* & t^* & 0 & 0 & 0 & 0 & 0 & 0 & 0 & 0 & \mathcal{E}_4 & 0 \\
 0 & 0 & 0 & t^* & t^* & 0 & 0 & 0 & 0 & 0 & 0 & 0 & \mathcal{E}_5
 \end{pmatrix}$$

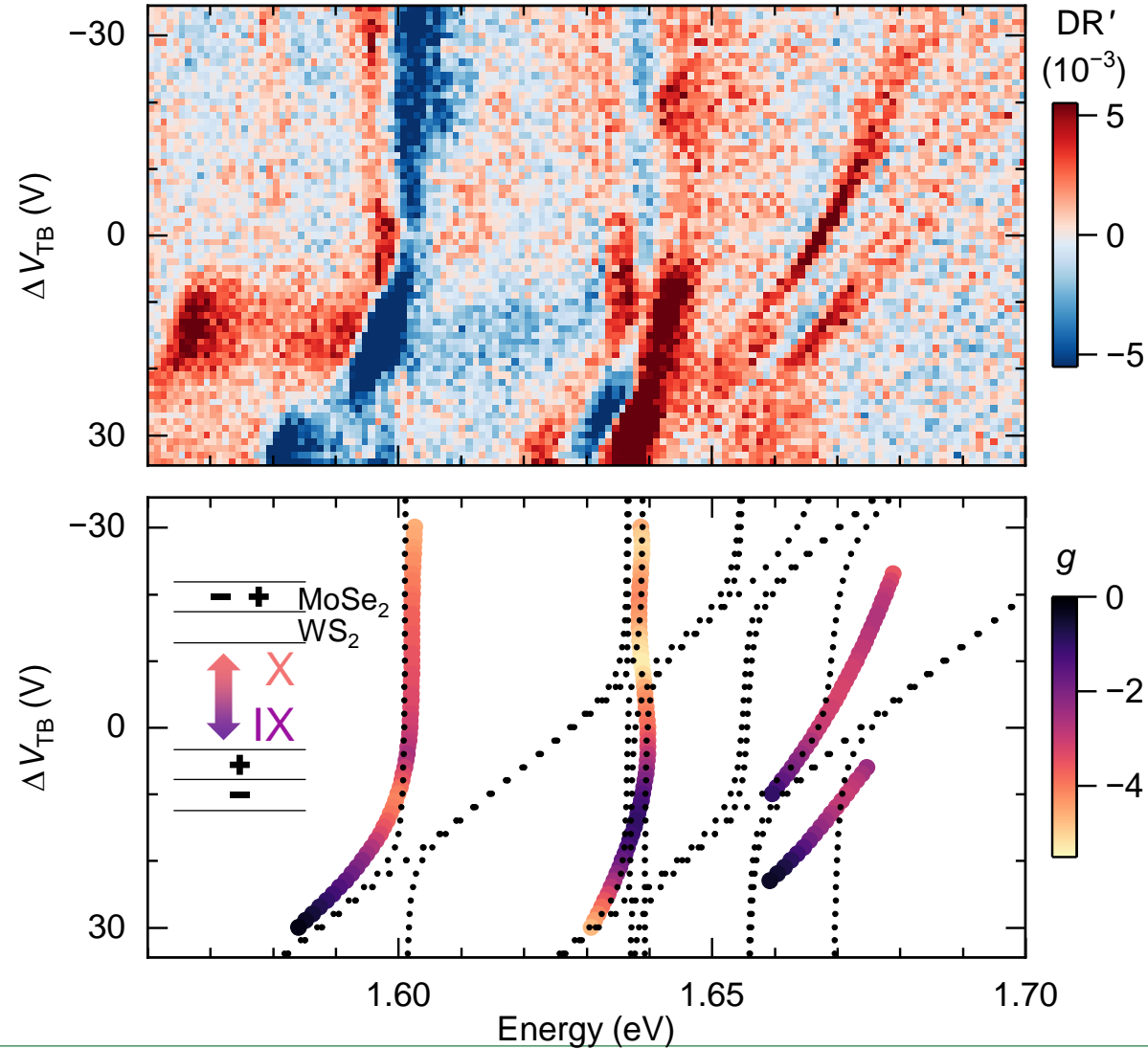
Fitting to E-field dependent data



Making the interlayer excitons visible



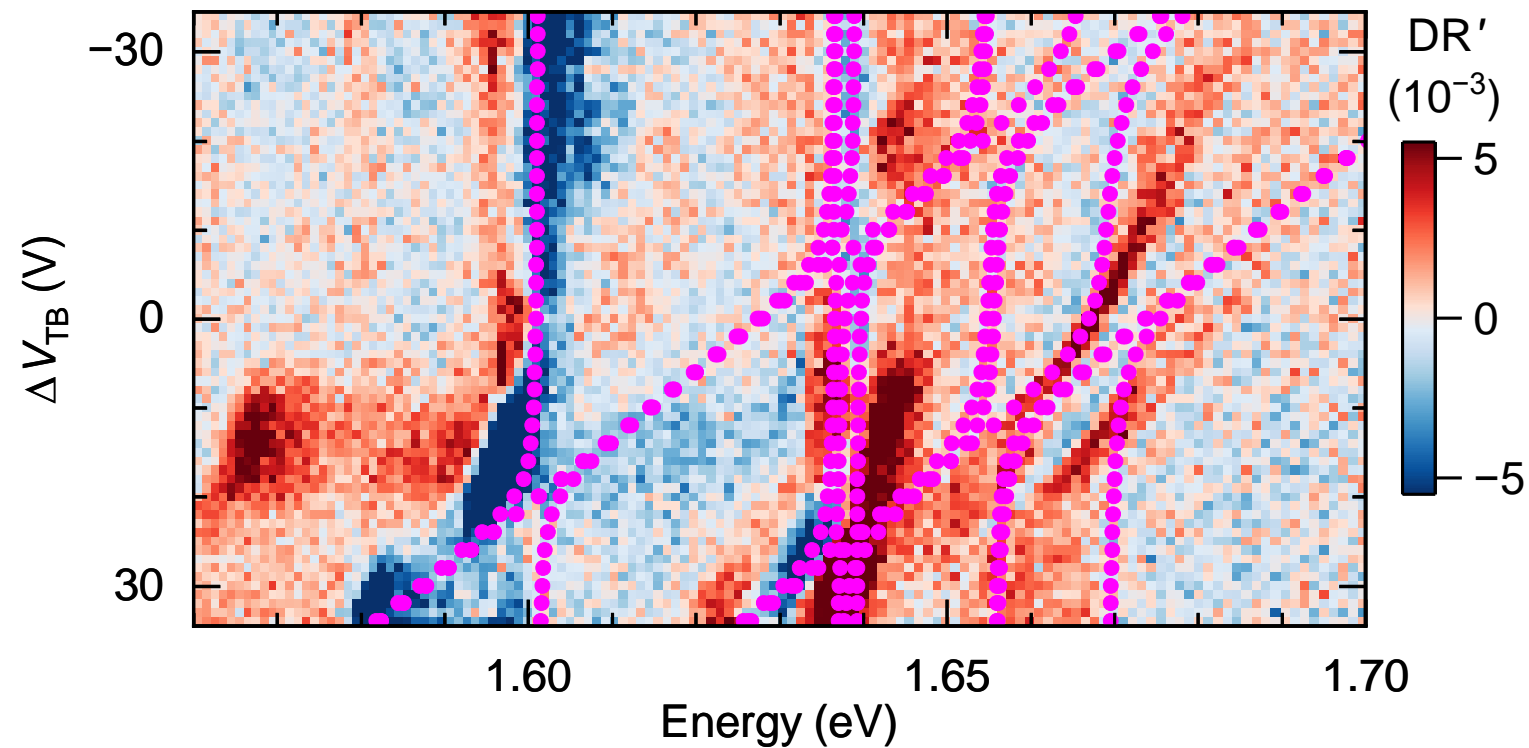
Making the interlayer excitons visible



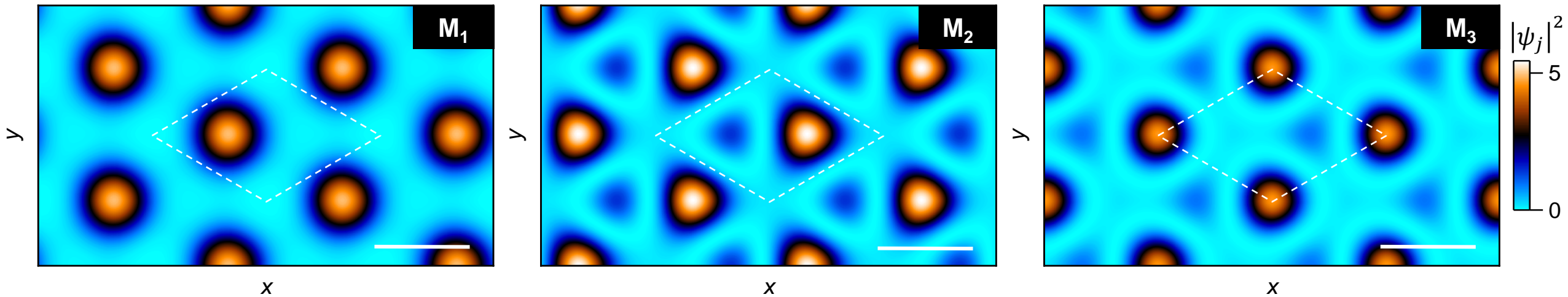
Dotted Lines: Eigenvalues of the Hamiltonian irrespective of the oscillator strength

Colors of the data points: deviations of the exciton Landé g-factor from the intralayer value $g = -4$

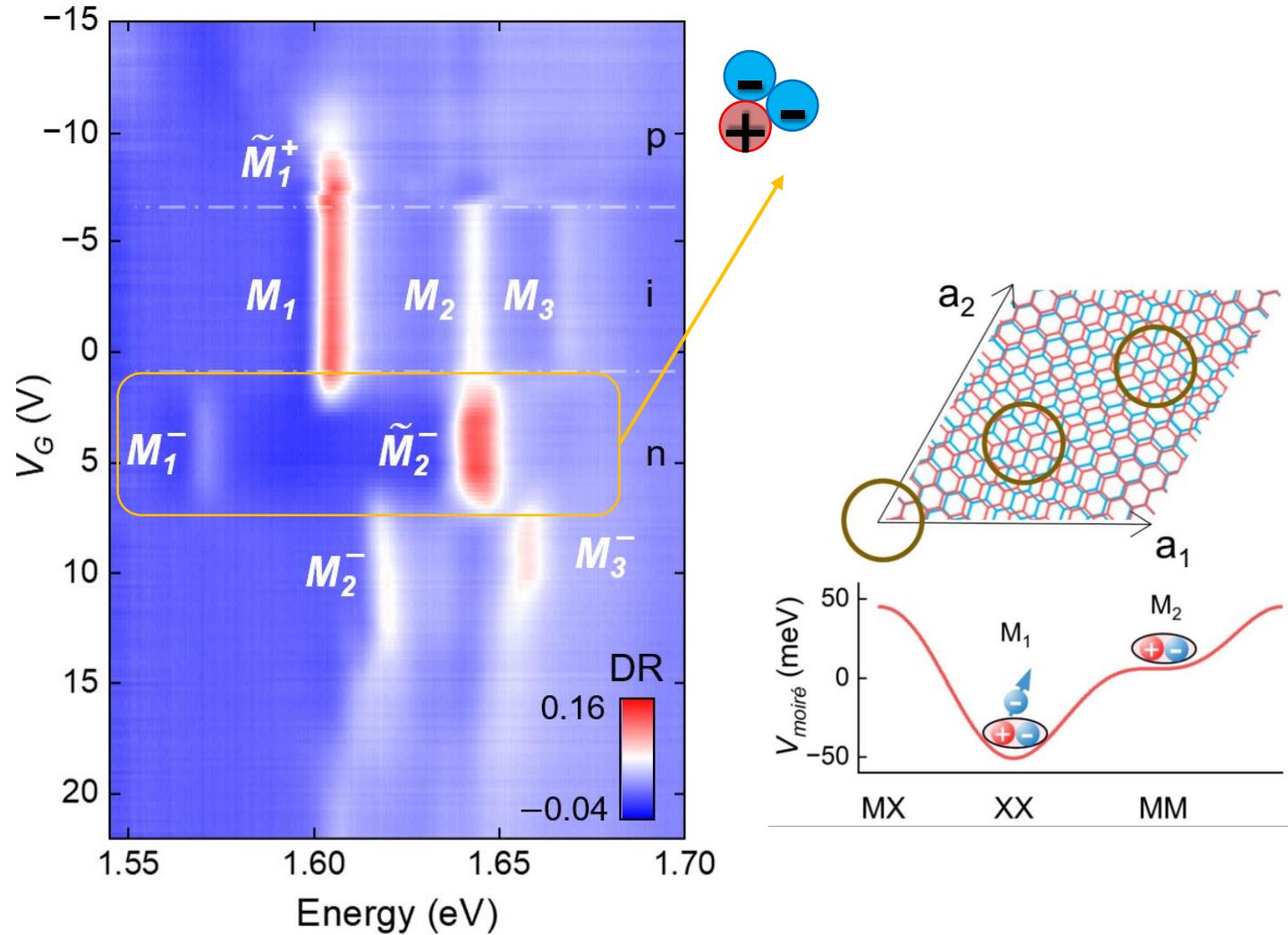
- At electric field ~ 0.05 V/nm the intra- and interlayer states exciton are resonant



Spatial distribution of bright moiré excitons



Charge doping effects on moiré excitons



- A simple effective model combining phenomenological moiré potentials with resonant interlayer hopping describes intra- and interlayer moiré excitons simultaneously;
- $\text{MoSe}_2/\text{WS}_2$ is of type I alignment, and the first IX state lies $\sim 30\text{meV}$ above the intralayer ground state exciton;
- A field of $\sim 0.05\text{ V/nm}$ is sufficient to bring the intra- and interlayer excitons into resonance, and beyond that type II alignment can be reached;
- Moiré excitons localize in real space and can act as reporters on band alignment or charge order.

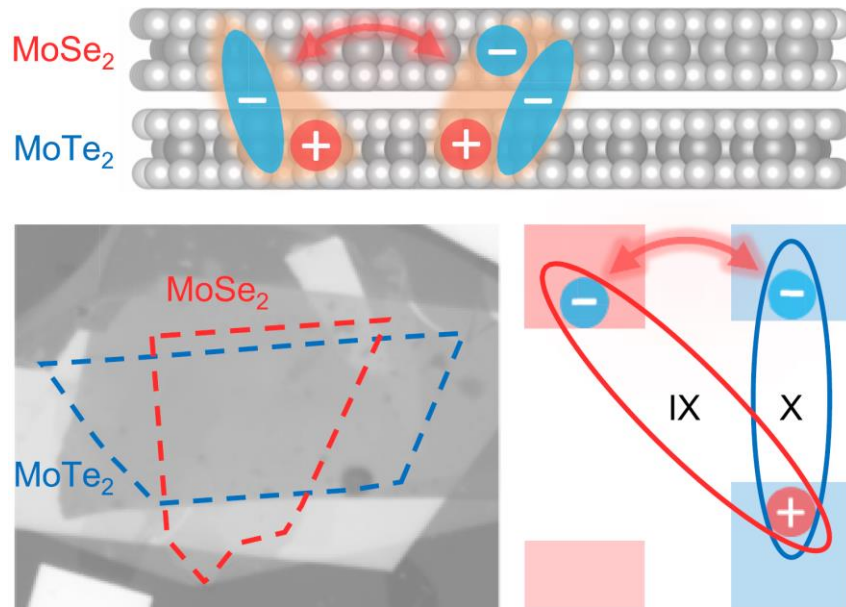
Editors' Suggestion

Field-Induced Hybridization of Moiré Excitons in $\text{MoSe}_2/\text{WS}_2$ Heterobilayers

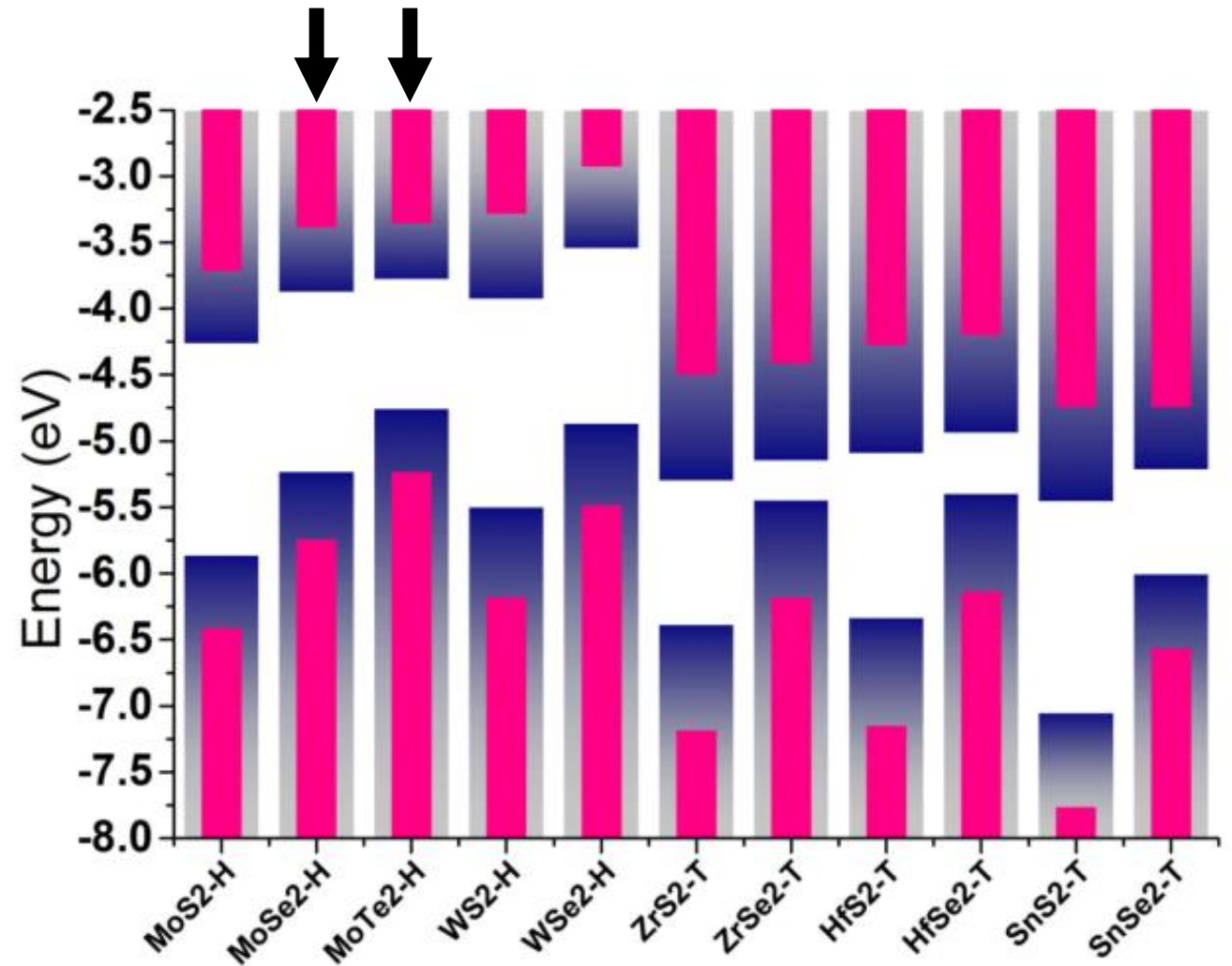
Borislav Polovnikov, Johannes Scherzer, Subhradeep Misra, Xin Huang, Christian Mohl, Zhijie Li, Jonas Göser, Jonathan Förste, Ismail Bilgin, Kenji Watanabe, Takashi Taniguchi, Alexander Högele, and Anvar S. Baimuratov
Phys. Rev. Lett. **132**, 076902 – Published 16 February 2024

Heterobilayer MoTe₂/ MoSe₂

- Lattice mismatch ~ 7%
- MoTe₂ and MoSe₂ have (almost) resonant CBs, allowing for intra- & interlayer exciton hybridization
- Holes are in MoTe₂ layer

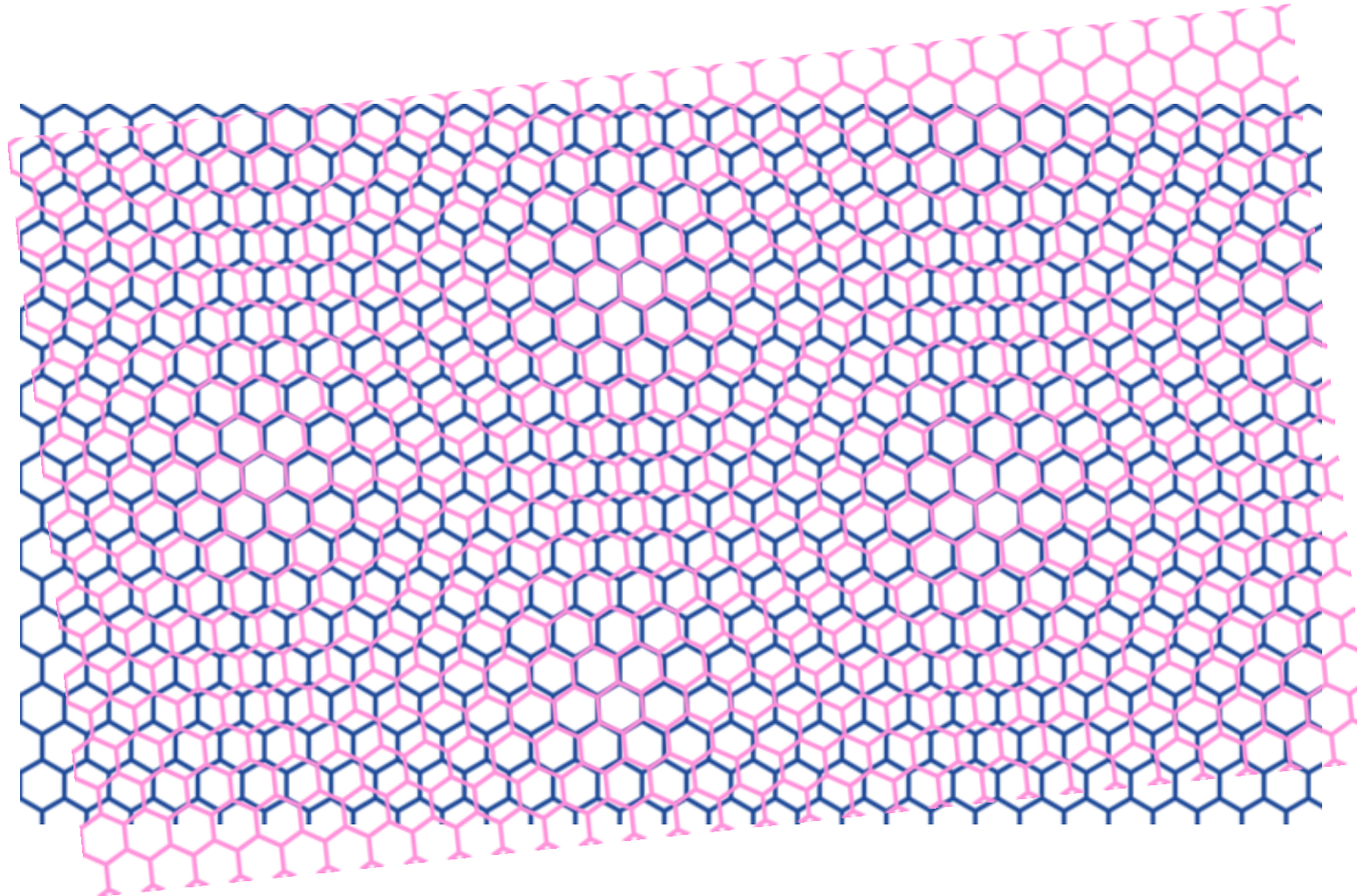


Zhao, Huang, ..., Högele, Baimuratov, Nano Lett. 24, 4917 (2024)

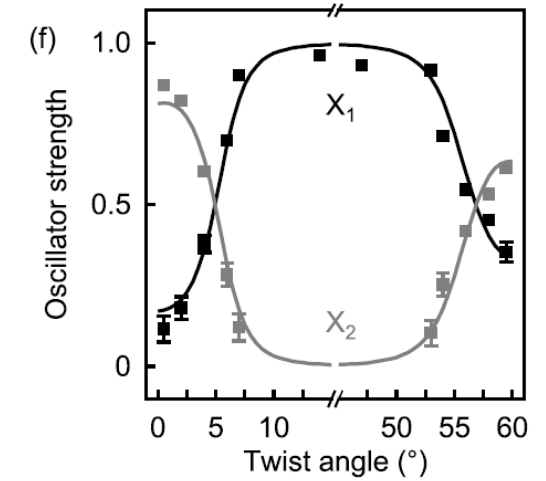
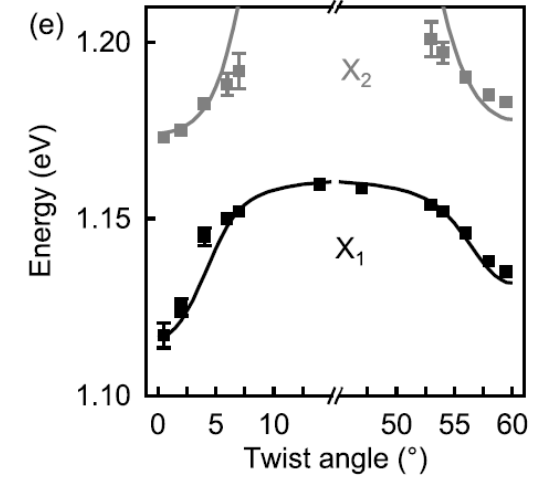
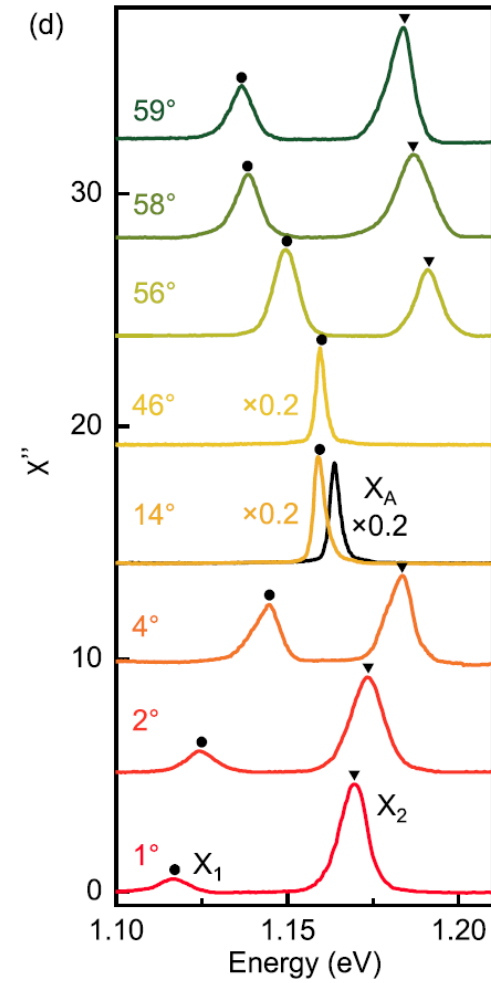
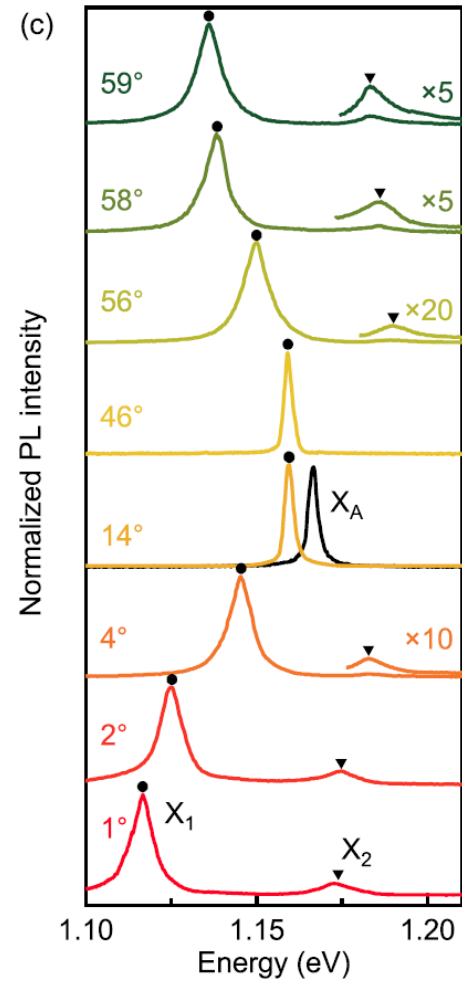
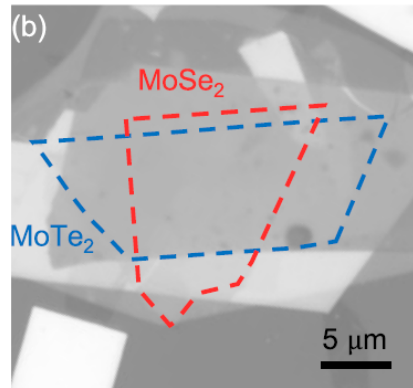
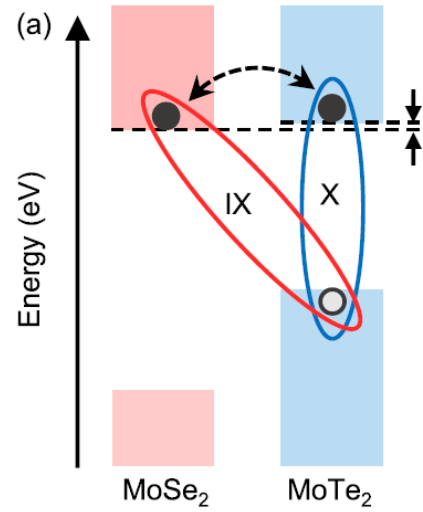


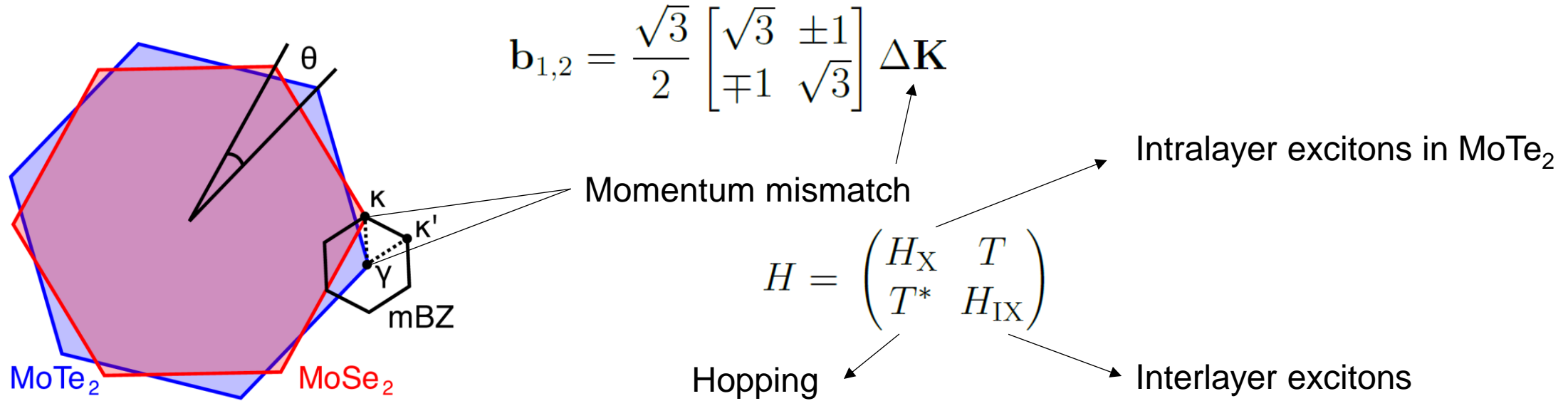
Zhang et al., 2D Mater. 4, 015026 (2016)

Heterobilayer $\text{MoTe}_2 / \text{MoSe}_2$



Heterobilayer MoTe₂/ MoSe₂





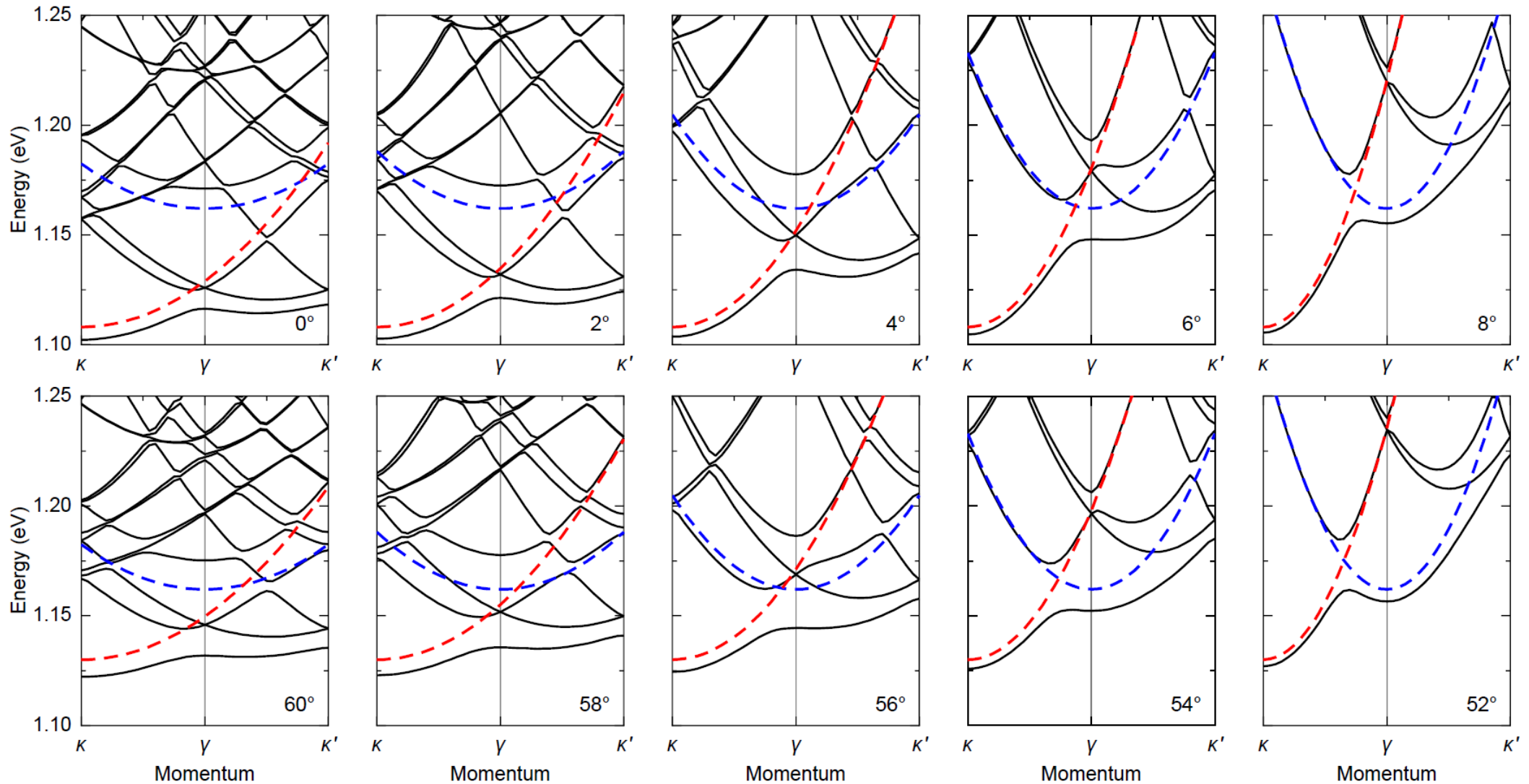
$$\langle X, \mathbf{k} + \mathbf{g}' | H_X | X, \mathbf{k} + \mathbf{g} \rangle = \delta_{\mathbf{g}, \mathbf{g}'} \left(E_X + \frac{\hbar^2 |\mathbf{k} + \mathbf{g}|^2}{2M_X} \right) + \sum_{j=1}^6 V_j \delta_{\mathbf{g}-\mathbf{g}', \mathbf{G}_j}$$

$$\langle IX, \mathbf{k}' + \mathbf{g}' | H_{IX} | IX, \mathbf{k}' + \mathbf{g} \rangle = \delta_{\mathbf{g}, \mathbf{g}'} \left(E_{IX} + \frac{\hbar^2 |\mathbf{k} + \mathbf{g}'|^2}{2M_{IX}} \right)$$

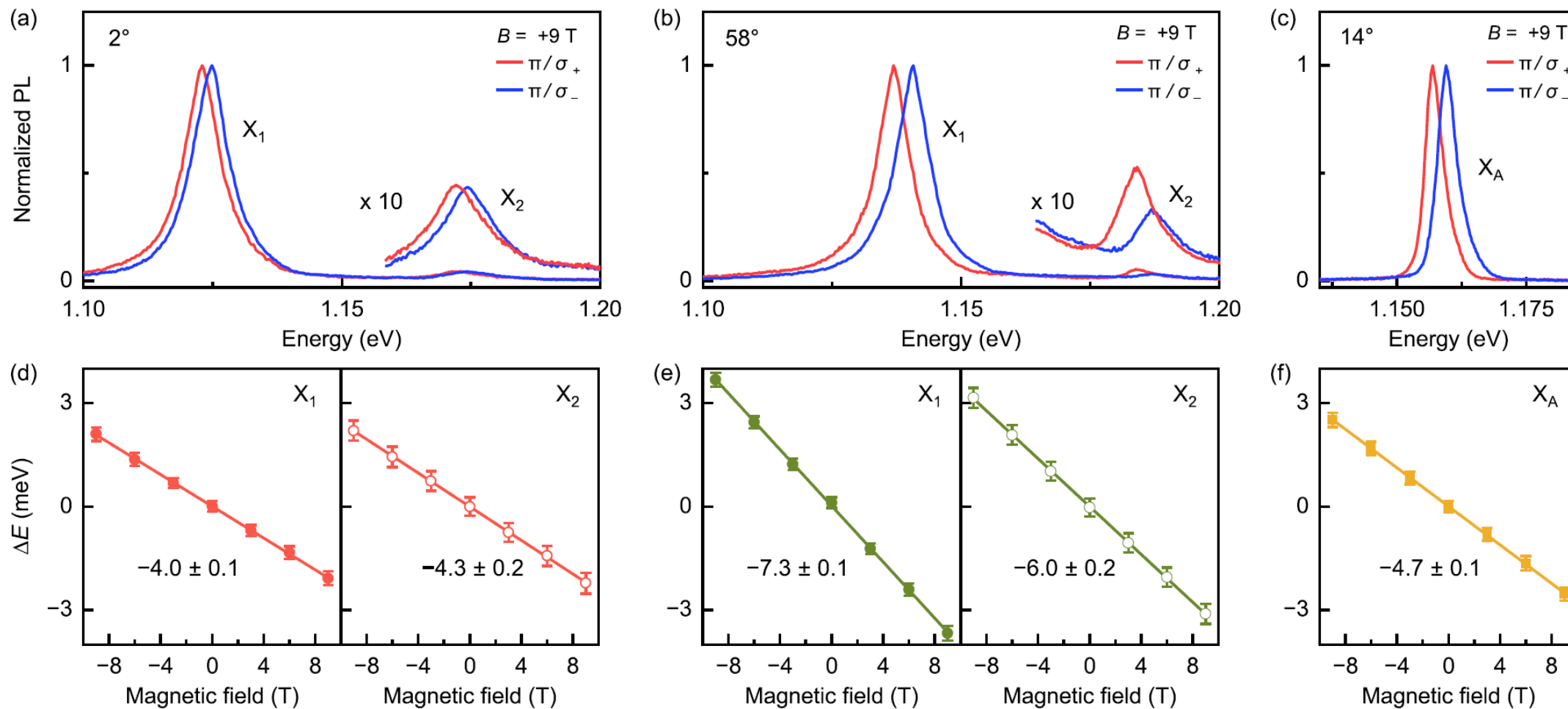
$$\langle IX, \mathbf{k}' + \mathbf{g}' | T | X, \mathbf{k} + \mathbf{g} \rangle = t (\delta_{\mathbf{k}+\mathbf{g}, \mathbf{k}'+\mathbf{g}'+\Delta \mathbf{K}} + \delta_{\mathbf{k}+\mathbf{g}, \mathbf{k}'+\mathbf{g}'+C_3^1 \Delta \mathbf{K}} + \delta_{\mathbf{k}+\mathbf{g}, \mathbf{k}'+\mathbf{g}'+C_3^2 \Delta \mathbf{K}})$$

Polovnikov, ... , Baimuratov, PRL 32, 076902 (2024)

Twist angle tuning



g-factors of hybrid excitons



g-factors of hybrid excitons

	m_c/m_0	m_{c+1}/m_0	m_v/m_0	Δ_{SO}	L_c	L_{c+1}	L_v
MoTe ₂	0.58	0.67	-0.68	69	1.586	1.204	3.872
MoSe ₂	0.55	0.63	-0.64	23	1.798	1.526	3.977

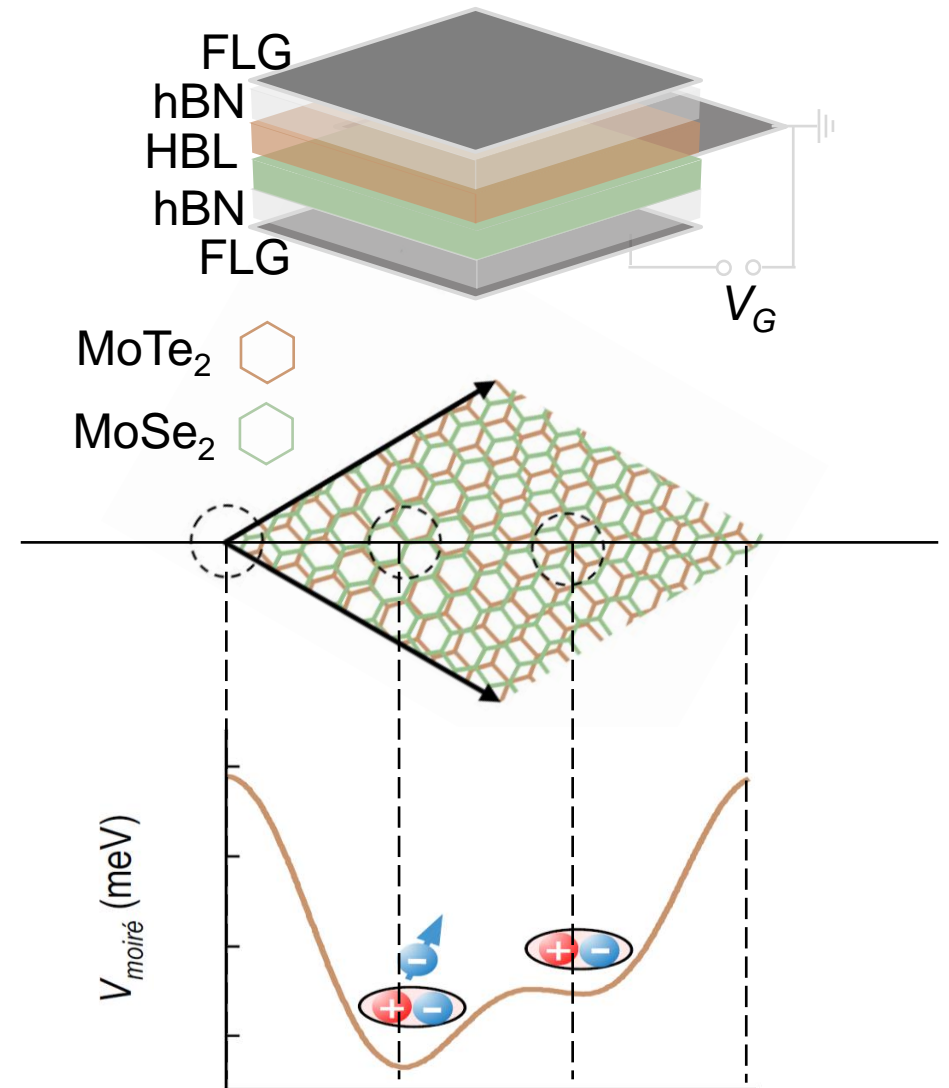
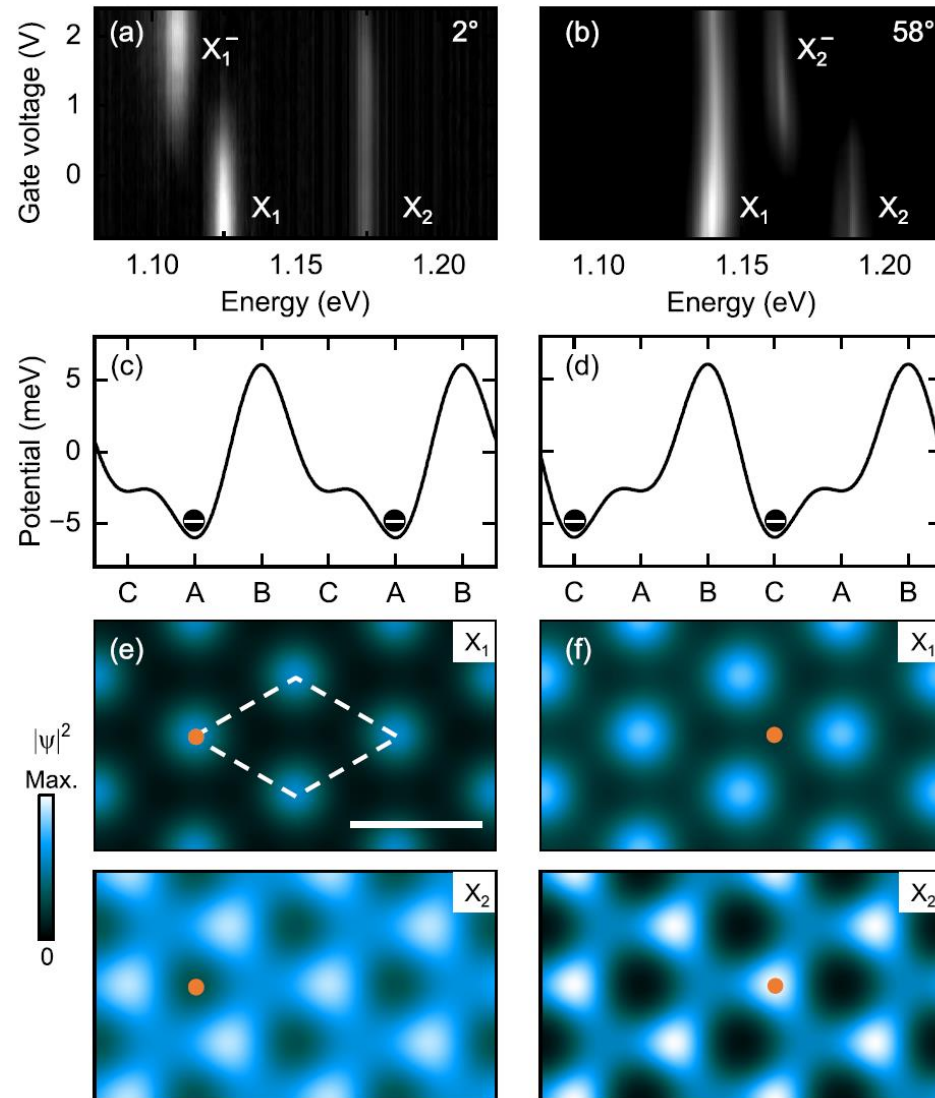
$$g_A = 2(L_c - L_v)$$

$$g_i^{(R)} = 2 \left(f_i^{(X)} L_c + f_i^{(IX)} L_{c'} - L_v \right)$$

$$g_i^{(H)} = 2 \left(f_i^{(X)} L_c - f_i^{(IX)} L_{c'+1} - L_v \right)$$

Twist angle	Exciton X ₁		Exciton X ₂	
	Exp.	Theory	Exp.	Theory
14°(R-type) and ML MoTe ₂	4.7	4.6	-	-
2° (R-type)	4.0	4.2	4.3	4.4
58° (H-type)	7.3	8.0	6.0	6.8

Doping and trion formation



- We study properties of $\text{MoTe}_2/\text{MoSe}_2$ heterobilayer and compare our data with the developed model;
- Heterobilayer $\text{MoTe}_2/\text{MoSe}_2$ demonstrates strong effect of hybridization without additional application of electric field;
- Our work provides fundamental understanding of hybrid moiré excitons and trions in $\text{MoTe}_2/\text{MoSe}_2$ heterobilayers and establishes the material system as a prime candidate for optical studies of correlated phenomena in moiré lattices.

NANO LETTERS

pubs.acs.org/NanoLett

Letter

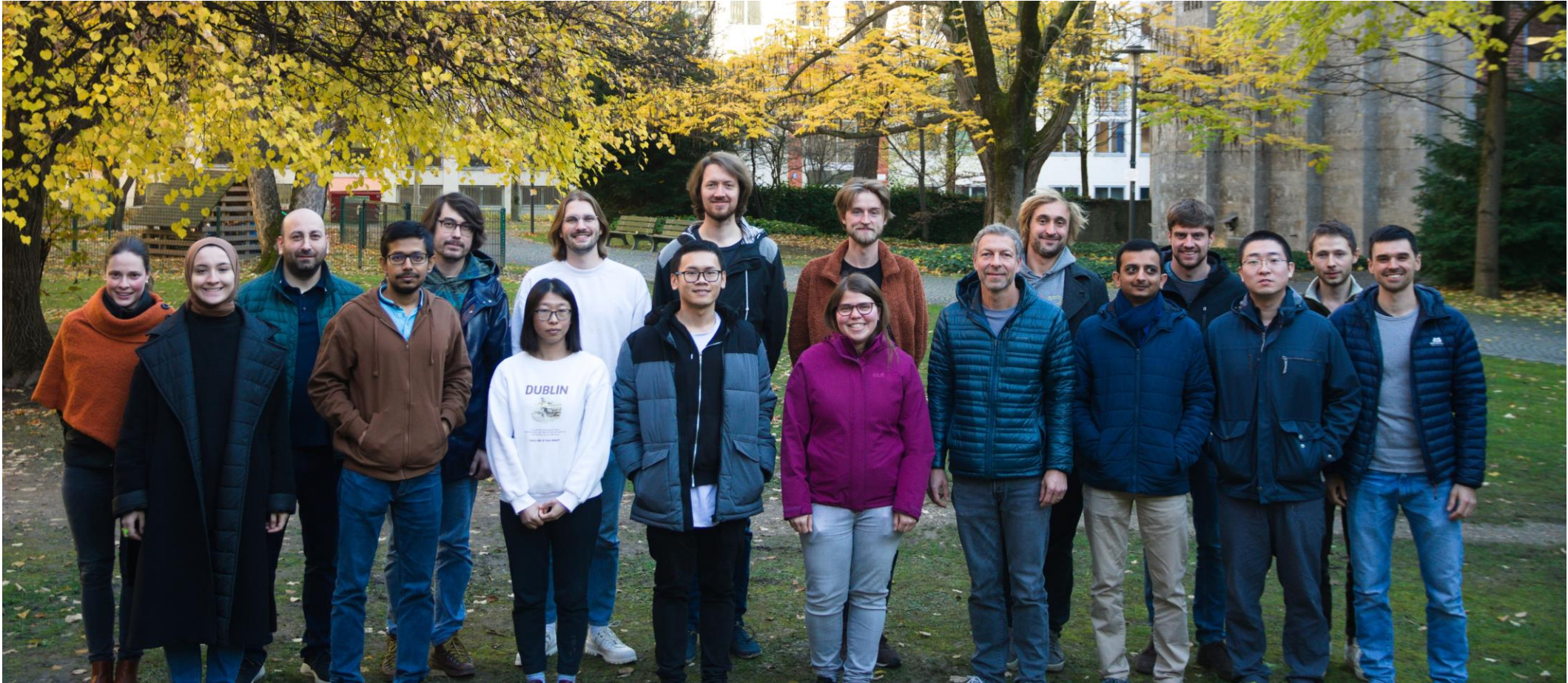
Hybrid Moiré Excitons and Trions in Twisted MoTe_2 – MoSe_2 Heterobilayers

Shen Zhao,[△] Xin Huang,^{*,△} Roland Gillen, Zhijie Li, Song Liu, Kenji Watanabe, Takashi Taniguchi, Janina Maultzsch, James Hone, Alexander Högele,^{*} and Anvar S. Baimuratov^{*}

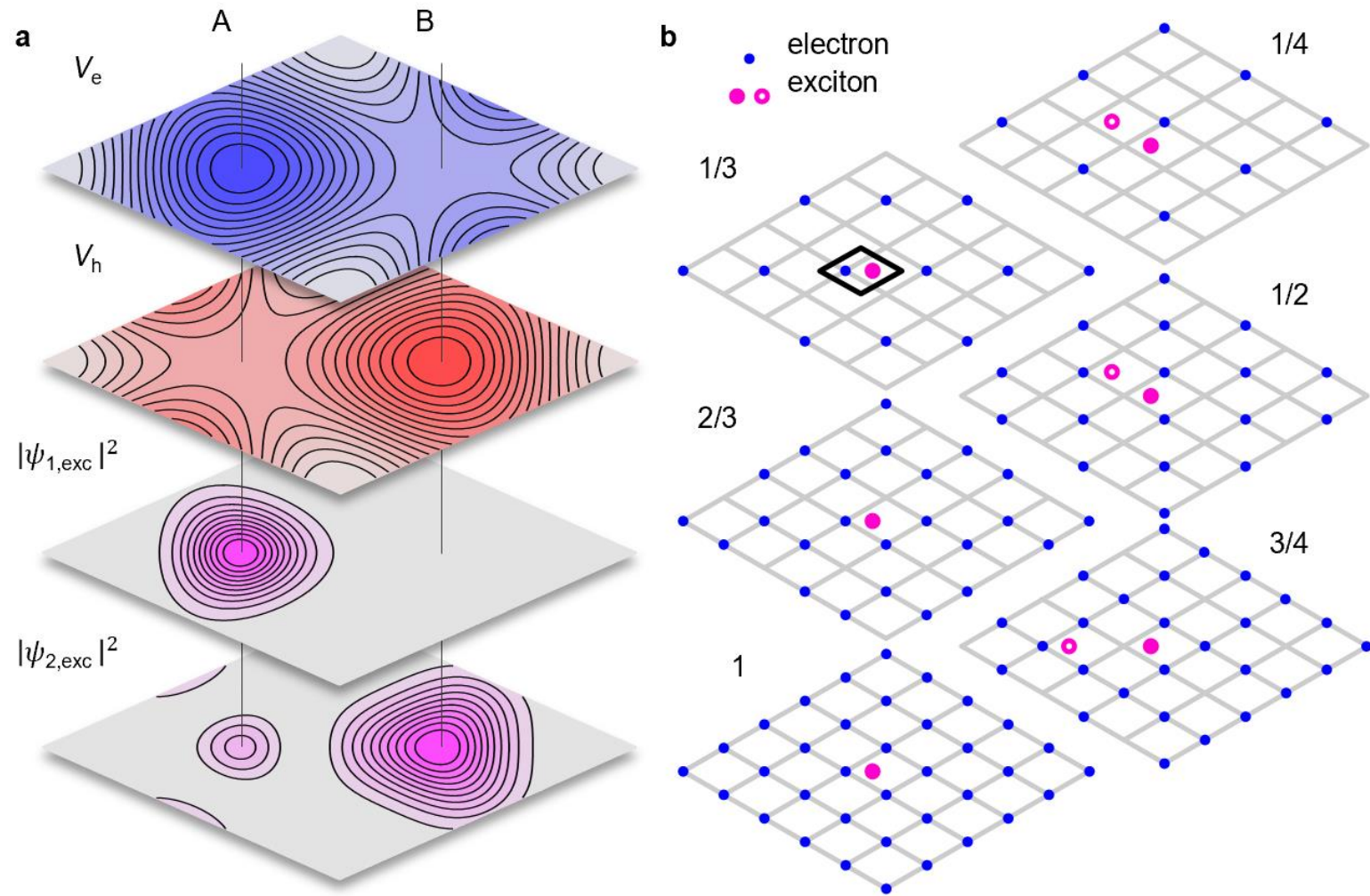
 Cite This: *Nano Lett.* 2024, 24, 4917–4923

 [Read Online](#)

THANKS!



Remote excitons as sensors of correlations



Magnetization of the electron lattice

